AD-A190 145 A NEW METHOD OF MEASURING MULTIGRADE OIL SHEAR ELASTICITY AND VISCOSITY A.. (U) WISCONSIN UNIV-MADISON DEPT OF ENGINEERING MECHANICS A S LODGE 1987 1/1

UNCLASSIFIED ARO-20015.7-EG DAAG29-84-K-0046 F/G 11/8 NL

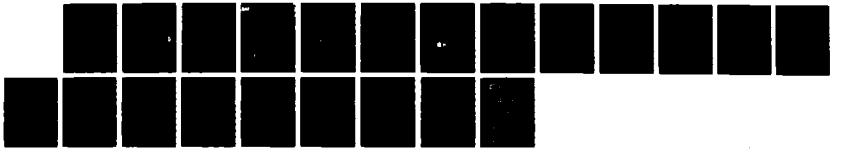

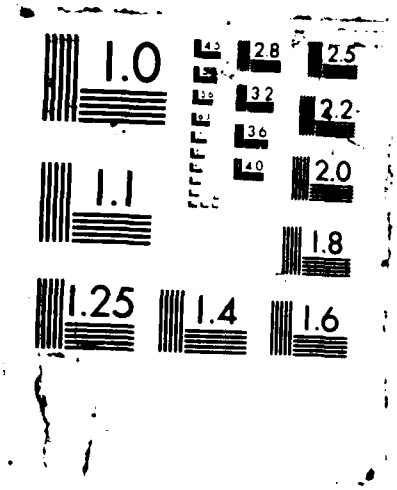
1.0
2.8
2.5
3.2
2.2
3.6
4.0
2.0
1.1
1.8
1.25
1.4
1.6

UNCLASSIFIED

SECURITY CLASSIFICATION OF THIS PAGE (When Data Entered)

(2)

| REPORT DOCUMENTATION PAGE | | READ INSTRUCTIONS BEFORE COMPLETING FORM |
|---|---|---|
| 1. REPORT NUMBER: 20815.7-EG | 2. GOVT ACCESSION NO.: N/A | 3. RECIPIENT'S CATALOG NUMBER: N/A |
| 4. TITLE (and Subtitle): A NEW METHOD OF MEASURING MULTIGRADE OIL SHEAR ELASTICITY AND VISCOSITY AT HIGH SHEAR RATES, SAE Technical Paper 872043, 1987 | | 5. TYPE OF REPORT & PERIOD COVERED: reprint |
| | | 6. PERFORMING ORG. REPORT NUMBER |
| AUTHOR(s): Arthur S. Lodge | | 8. CONTRACT OR GRANT NUMBER(s): DAAG29-84-K-0046 |
| PERFORMING ORGANIZATION NAME AND ADDRESS: Department of Engineering Mechanics, University of Wisconsin-Madison, Madison, WI 53706 | | 10. PROGRAM ELEMENT, PROJECT, TASK AREA & WORK UNIT NUMBERS |
| CONTROLLING OFFICE NAME AND ADDRESS: U. S. Army Research Office, Post Office Box 12211, Research Triangle Park, NC 27709 | | 12. REPORT DATE |
| | | 13. NUMBER OF PAGES: 16 |
| MONITORING AGENCY NAME & ADDRESS (if different from Controlling Office) | | 15. SECURITY CLASS. (of this report): Unclassified |
| | | 15a. DECLASSIFICATION/DOWNGRADING SCHEDULE |

AD-A190 145

DTIC FILE COPY

16. DISTRIBUTION STATEMENT (of this Report)

Approved for public release; distribution unlimited.

DTIC ELECTE FEB 01 1988 S D E

17. DISTRIBUTION STATEMENT (of the abstract entered in Block 20, if different from Report)

NA

18. SUPPLEMENTARY NOTES

The view, opinions, and/or findings contained in this report are those of the author(s) and should not be construed as an official Department of the Army position, policy, or decision, unless so designated by other documentation.

19. KEY WORDS (Continue on reverse side if necessary and identify by block number)

lubrication, oil shear elasticity, first normal stress difference, oil viscosity, Stressmeter, high shear rate

20. ABSTRACT (Continue on reverse side if necessary and identify by block number)

Recent journal bearing oil film thickness data (1) strongly suggest that, in order to develop minimum-viscosity multigrade oils for maximizing fuel economy, it is not enough to examine viscosity $\eta$ alone, even at 150 °C at a shear rate $\dot{\gamma} = 10^6\ s^{-1}$: it is essential also to examine a certain kind of shear elasticity, of which one measure is the *first normal stress difference* $N_1$ in shear flow. Within a group of isoviscous multigrade oils, $N_1$ values can differ significantly; for 10W-40 and 15W-40 oils, an average of 75% of

(over)

DD FORM 1 JAN 73 1473 EDITION OF 1 NOV 65 IS OBSOLETE

UNCLASSIFIED

SECURITY CLASSIFICATION OF THIS PAGE (When Data Entered)

20 (continued)

the minimum oil film thickness can be attributed to $N_1$ (1). Here we describe (a) the method used in (1) to obtain high $\dot{\gamma}$ $N_1$ data, (b) an increase in the $N_1$-measurement upper limit $\dot{\gamma}_{max}$ from $3 \times 10^5$ $s^{-1}$ to $10^6$ $s^{-1}$ (where $\eta \approx 10$ cP), and (c) an increase in the $\eta$-measurement $\dot{\gamma}_{max}$ to $5 \times 10^6$ $s^{-1}$. This is close to the $\dot{\gamma}_{max}$ value found in (1) and is five times greater than that at present attainable with other commercially available viscometers.

1. Bates, T. W., B. Williamson, J. A. Spearot, C. K. Murphy, SAE Paper No. 860376 (1986).

The Engineering Society For Advancing Mobility Land Sea Air and Space®

400 COMMONWEALTH DRIVE WARRENDALE, PA 15096

# SAE Technical Paper Series

872043

# A New Method of Measuring Multigrade Oil Shear Elasticity and Viscosity at High Shear Rates

**A. S. Lodge**
University of Wisconsin-Madison
Engine & Rheology Research Centers



International Fuels and Lubricants Meeting and Exposition
Toronto, Ontario
November 2-5, 1987

*All SAE papers are abstracted and indexed in the SAE Global Mobility Database*

SAE GLOBAL MOBILITY DATABASE



**ISSN 0148-7191**

872043

# A New Method of Measuring Multigrade Oil Shear Elasticity and Viscosity at High Shear Rates

**A. S. Lodge**
University of Wisconsin-Madison
Engine & Rheology Research Centers

**ABSTRACT**

Recent journal bearing oil film thickness data (1)* strongly suggest that, in order to develop minimum-viscosity multigrade oils for maximizing fuel economy, it is not enough to examine viscosity $\eta$ alone, even at 150C at a shear rate $\dot{\gamma} = 10^6 s^{-1}$: it is essential also to examine a certain kind of shear elasticity, of which one measure is the *first normal stress difference* $N_1$ in shear flow. Within a group of isoviscous multigrade oils, $N_1$ values can differ significantly; for 10W-40 & 15W-40 oils, an average of 75% of the minimum oil film thickness can be attributed to $N_1$ (1). Here we describe (a) the method used in (1) to obtain high-$\dot{\gamma}$ $N_1$ data; (b) an increase in the $N_1$-measurement upper limit $\dot{\gamma}_{max}$ from $3\ 10^5 s^{-1}$ to $10^6 s^{-1}$ (where $\eta$ = 10cP); & (c) an increase in the $\eta$-measurement $\dot{\gamma}_{max}$ to $5\ 10^6 s^{-1}$. This is close to the $\dot{\gamma}_{max}$ value found in (1) & is 5 times greater than that at present attainable with other commercially available viscometers.

IT IS WELL KNOWN THAT, in the first instance, polymers were added to lubricating oils in order to reduce the temperature dependence of viscosity. However, the addition of polymer has other effects, notably the creation of a group of non-Newtonian rheological properties that can collectively be termed *elastic*, which are not exhibited by single grade oils (containing no polymeric additives). The possible beneficial effects of oil elasticity on journal bearing lubrication have been considered for over 30 years (2-6); until recently, the experimental investigations (mostly of wear) have been somewhat inconclusive.

*Numbers in parentheses (not preceded by Eq.) refer to the REFERENCES section at the end of the paper.

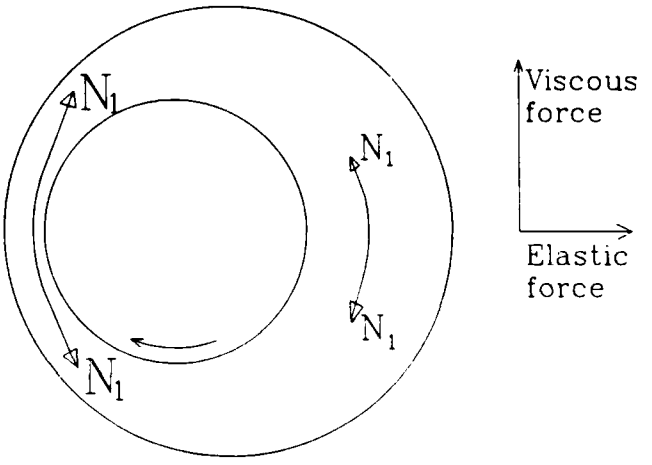


FIGURE 1 Addition of polymer to lubricating oil generates an elastic contribution $N_1$ to the state of stress in shear flow in full film hydrodynamic lubrication in a journal bearing. The elastic contribution has the nature of a tensile hoop stress acting tangentially to the shear lines. Where the gap is smaller, the shear rate & $N_1$ values are larger. The $N_1$ distribution thus gives a resultant force on the journal, which acts in line with the minimum film thickness diameter in a direction tending to increase the minimum film thickness.

For multigrade oils in shear flow, the state of stress in a liquid element can be regarded (7) as a superposition of an isotropic pressure p, a shear stress $\sigma$, & first & second normal stress differences $N_1$ & $N_2$. The rate at which surface tractions do work on the element is equal to $\sigma\dot{\gamma}$ per unit volume & does not depend on $N_1$. For most non-Newtonian polymeric liquids, $N_1 > 0$. $N_1$ is related to elastic recovery at constant volume (8). $N_1^2/\sigma$, one definition of an oil shear modulus, is of the order $10^2$-$10^4$Pa & is a quantity distinct from the bulk modulus (typically of the order $10^9$-$10^{10}$Pa).

Fig.1 shows one possible mechanism whereby,

0148-7191/87/1102-2043$02.50

for the case of full film hydrodynamic lubrication, oil elasticity can, at least in principle, generate an additional force on the journal in a direction tending to increase the minimum oil film thickness. This elastic force contribution is at right angles to that due to viscosity & is of particular value because, being associated solely with $N_1$, the first normal stress difference (a conservative contribution to stress), no energy is consumed in its generation. If, therefore, significant elastic effects can be generated & maintained under practical operating conditions, it should be possible to reduce oil viscosity while maintaining acceptable oil film thicknesses. If journal bearing failure is a critical factor where oil viscosity reduction is to be considered in relation to complete engine performance, it is reasonable to hope that acceptable lower-viscosity multigrade oils could be formulated & hence that energy savings could result.

In shear flow between vertical cylinders in relative rotation, $N_1$ acts like a hoop stress giving rise to the "Weissenberg Effect" in which the liquid climbs up the inner cylinder. If the cylinders are coaxial, this hoop stress distribution has rotational symmetry about the common axis & so gives no resultant force contribution in planes normal to the cylinders. In a journal bearing under load, the journal & bearing are not coaxial (fig.1) & there is a resultant "elastic" force contribution from the asymmetric $N_1$ distribution.

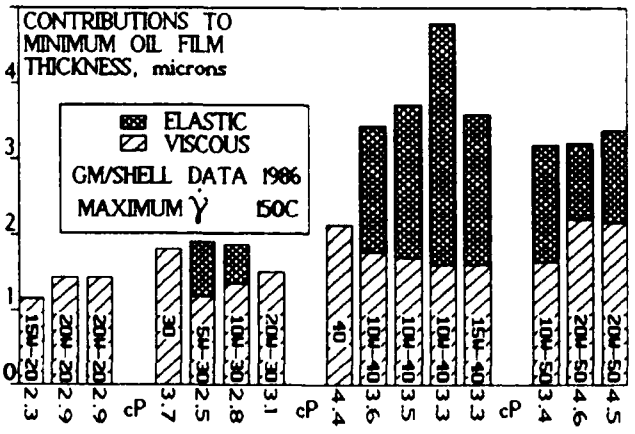


**FIGURE 2** The above recent GM/Shell data (1) show that, in order to correlate measured values of minimum oil film thickness in a front main bearing of a V-6 engine running at 3000 rpm with rheological properties of the oils, it is necessary to include the elastic quantity $N_1$ as well as the viscosity $\eta$. Oil viscosities in mPas (cP) are given on the bottom line. On average, at equal high-temperature, high-shear-rate viscosities, the minimum film thicknesses for the SAE 10W-40 & 15W-40 elastic oils are 75% greater than those for the SAE 40 inelastic oil.

Recently (1), electrical resistance probes were used to measure oil film thickness in a V-6 front main bearing at 3000 rpm. A concentric cylinder apparatus was used to measure viscosity. A new instrument, the LODGE STRESSMETER(R) FOR HIGH SHEAR RATES, was used to measure $N_1$ for shear rates up to $3\ 10^5 s^{-1}$ & temperatures up to 60C; extrapolation was used in order to extend the range to 150C & $6\ 10^6 s^{-1}$, the highest estimated shear rate used. For the set of 2 single grade & 13 multigrade oils investigated, inclusion of an $N_1$ term in a regression equation for the minimum oil film thickness gave an increase in the correlation coefficient $R^2$ from 0.15 to 0.70 compared with the case in which viscosity alone was used. Some results (from Table 12 of (1)) are presented in fig.2. The authors conclude that

"***multigrade oils result in thicker oil films than single grades at equal high-temperature, high-shear-rate viscosities;...film thicknesses for the SAE 10W-40 & 15W-40 oils are, on average, 75% greater than the SAE 40 single grade oil.***" (our italics)

The importance of elastic contributions shown by these results is surprising in view of theoretical estimates (4-6) which suggest that values of the stress ratio $N_1/\sigma$ (where $\sigma$ denotes the shear stress) would need to be of the order of several hundred to make the fig.1 $N_1$ contribution comparable in magnitude with the viscous contribution. Since the measured values of $N_1/\sigma$ were below 10, the observed strong correlation between film thickness & $N_1$ data is unexpected and has yet to be explained.

In seeking an explanation, possible factors to be considered include the following: the maximum value 0.96 of the eccentricity ratio (9) in the measurements was much greater than the values used in the calculations; squeeze film behavior associated particularly with dynamic loading of short bearings may play a significant role (10); polymer additives might affect cavitation & boundary lubrication; $N_1$ may play the sole role of a sensitive detector of high MW polymer or of polymer-polymer interactions, & the polymer itself may act (in some as yet unknown manner) to increase the minimum film thickness. Examples are known (11, 12) in which polymer MW changes affect $N_1$ but not $\eta$.

The statistical significance of the correlation between $N_1$ & minimum film thickness is independent of the fact that we have as yet no adequate hypothesis for a mechanism which might account for this correlation.

Whatever the mechanism may be, it seems to be beyond reasonable doubt that the GM/Shell results (1) establish two important facts in regard to journal bearing lubrication: oil elasticity can play as important a role as oil viscosity, & shear rates much higher than the value $10^6 s^{-1}$ (at present under committee consideration) occur in practical bearing conditions. The highest shear rate in the GM/Shell studies was $5.6\ 10^6 s^{-1}$. Exxon studies (13) show that even higher shear rates (above $10^7 s^{-1}$) can occur during acceleration.

In the present paper, we give information about the method used by Shell to measure $N_1$ for

multigrade oils; we describe recent attempts to extend the range of $N_1$ measurement to higher shear rates & temperatures in order to obviate extrapolation; & we give preliminary results which suggest that viscosities near 2 cP can be measured up to $\dot{\gamma} = 5\ 10^6 s^{-1}$. It is better to avoid extrapolation if possible, particularly for block copolymer additives for which morphological changes occur at certain temperatures.

## ELASTIC LIQUID HOLE PRESSURES

When a liquid undergoes shear flow between parallel walls, the stream surfaces are plane. If one wall has a small transverse slot, the stream surfaces near the slot mouth are curved in the sense illustrated in fig.3. This hole-generated curvature combined with a shear-generated $N_1$ distribution gives rise to a positive *hole pressure* $P^* := P_1 - P_2$, where $P_1$ denotes the pressure exerted on the wall opposite the slot center & $P_2$ denotes the pressure at the slot base. A force balance on the liquid contained within the dashed lines of fig.3 shows that $P^*$ will increase with $N_1$.

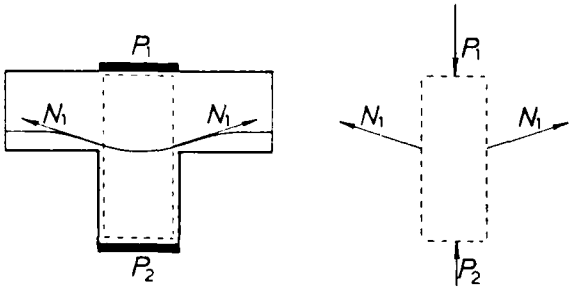


FIGURE 3 Hole-induced curvature of the stream surfaces near the mouth of a transverse slot combined with a shear-flow-induced $N_1$ distribution generate a positive value of $P^* = P_1 - P_2$. Measurements of $P^*$ are here used to determine $N_1$ for multigrade oils at high shear rates.

In practice, there are additional contributions to $P^*$ arising from inertial forces (because the slot has a finite width b) & from the response of the flush-mounted transducer to a non-uniform pressure (because this transducer has a finite width (14) & may, in addition, be imperfectly aligned with the slot mouth). For small values of Reynolds number Re & sufficiently small flush transducer diaphragm deflections, it is reasonable to assume that the three contributions are additive & mutually independent, so that we may write

$$P^* = P^*_f + P^*_N + P^*_e, \qquad (1)$$

where $P^*_f$, the flush transducer finite width contribution, may, for a given transducer & die geometry, be assumed to be determined by the wall shear stress $\sigma$ and, possibly, the temperature; $P^*_N$, the inertial contribution, may be assumed to be a product of $\sigma$ & some function of Re; $P^*_e$, the "elastic" contribution, is expected to be a positive monotonic increasing function of $N_1$. Re is defined here by the equation

$$Re = \rho b h \dot{\gamma}/(4\eta), \qquad (2)$$

where $\rho$ & $\eta$ denote the liquid density & viscosity, $\dot{\gamma}$ denotes the shear rate at the wall at a location unperturbed by the hole, b denotes the slot mouth dimension parallel to the main flow direction, & h denotes the wall separation.

A "STRESSMETER" is a slit die rheometer (fig.4) with which the hole pressure $P^*$, the shear stress $\sigma$, & the shear rate $\dot{\gamma}$ can be measured. Here we consider only the case in which the hole cross section is a narrow rectangle (a transverse slot); circular holes have also been used (11,14,15).

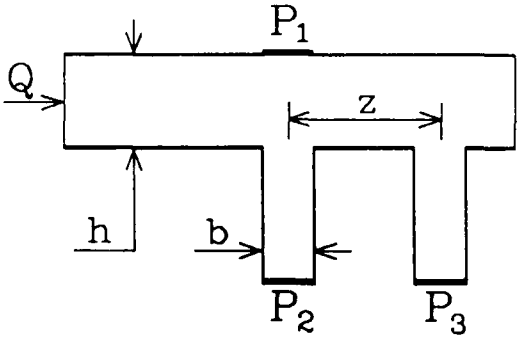


FIGURE 4 Schematic diagram of a central section of a STRESSMETER die. Pressures $P_1$, $P_2$, & $P_3$ are measured by means of one flush-mounted & two hole-mounted transducers. The shear stress $\sigma$ and the first normal stress difference $N_1$ are determined from $P_2 - P_3$ & $P_1 - P_2$, respectively. The flow rate Q is determined from the rate of rise of test liquid discharging into an output cylinder (fig.5). The viscosity is determined from $\sigma$ & Q.

The "HPBL theory" (11,15-17) relating $P^*_e$ & $N_1$ is not as well established as the theory for measuring $N_1$ in a cone-plate rheometer. The HPBL theory for a transverse slot gives equations:

$$N_1 = 2nP^*_e, \qquad (3)$$

$$n = d(\log P^*_e)/d(\log \sigma). \qquad (4)$$

Here & throughout, $N_1$, $\sigma$, & $\dot{\gamma}$ denote values at the die wall in a fully developed flow region where perturbations from the slots' presence are negligible. For the particular case in which $N_1$ is proportional to $\sigma^2$ over a range which includes zero, $n = 2$ & Eq.(3) gives $N_1 = 4P^*_e$; if $b \ll h$ & $P^*_N = 0$ (a low Re limit), this agrees with the result of an approximate analysis (18) for a particular form of constitutive equation (the "Second Order Fluid"); for multigrade oil & many other applications, this simple equation is too restrictive, & Eq.(3) is more useful. For a circular hole, Eq.(3) is replaced by the similar equation $N_1 - N_2 = 3nP^*_e$.

Extensive tests of these equations, made by comparing $N_1$ & $N_1 - N_2$ values obtained from them and from measurements made with absolute rheometers, have been reported elsewhere (11,15) for several polymeric liquids. The curious result is

that, within the scatter of measurement (usually about ±10% or better), the range of validity of the HPBL equations extends rather far beyond the range of validity of assumptions used in their derivation (16,17). The explanation of this fortunate result is as yet unknown, but this need not prevent us from exploiting it. Numerical simulations are also being used to investigate the validity of Eq.(3) for various constitutive equations (19,20).

## THE LODGE STRESSMETER(R) FOR HIGH SHEAR RATES

A schematic diagram of a central section of the STRESSMETER die is given in fig.4. Located far enough downstream from the die entrance, so that entrance flow disturbances are negligible, are two small, deep, parallel, transverse slots of width $b < h$, the die height. Pressures $P_2$ & $P_3$ at the bases of these slots are measured by transducers $T_2$ & $T_3$. With its effective center located as close as possible to the $P_2$ hole centerline produced, a third transducer $T_1$ is mounted flush with the die wall opposite the slot mouths. Compressed nitrogen or air drives the test liquid from a drive cylinder through the die & into an output cylinder (figs.5,6) in whose base is a liquid-filled hole connected to a fourth transducer $T_4$ whose pressure reading time derivative gives the flow rate Q.

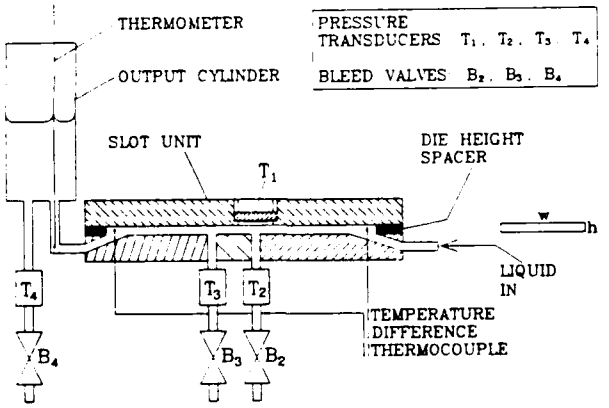


**FIGURE 5** Schematic diagram of a STRESSMETER slot unit, showing a flush-mounted transducer $T_1$, slot-mounted transducers $T_2$, $T_3$, temperature-difference thermocouple, downstream thermometer, output cylinder, & flow rate transducer $T_4$. Typical die dimensions are given in Table 1.

Fine-wire thermocouples in contact with the flowing test liquid are located up- & downstream from the die in order to get a rough measurement of the temperature rise caused by the work done in forcing the liquid through the die; this rise usually does not exceed about 1 deg. C, which is negligible for most multigrade oil applications. The measurement temperature is determined from the reading of a platinum resistance thermometer in the output stream between the die exit & the output cylinder base; this is expected to give something close to a cup mixing temperature.

For isothermal shear flow through a slit die (21), the shear stress $\sigma$, shear rate $\dot{\gamma}$, & viscosity $\eta$ are determined from the equations

$$\sigma = h(P_2 - P_3)/(2z); \quad (5)$$

$$\dot{\gamma} = 2(2 + m)Q/(wh^2); \quad (6)$$

$$m = d(\log Q)/d(\log \sigma); \quad (7)$$

$$\eta = \sigma/\dot{\gamma}. \quad (8)$$

Here, w denotes the die width & z denotes the distance between slot centers measured parallel to the main flow direction. Eqs.(6) & (7) embody the well known slit-die analog of the Weissenberg-Rabinowitsch correction for homogeneous liquids for which $\eta$ varies with $\dot{\gamma}$. When $\eta$ is independent of $\dot{\gamma}$, $m = 1$ & Eq.(6) gives $\dot{\gamma} = 6Q/(wh^2)$.

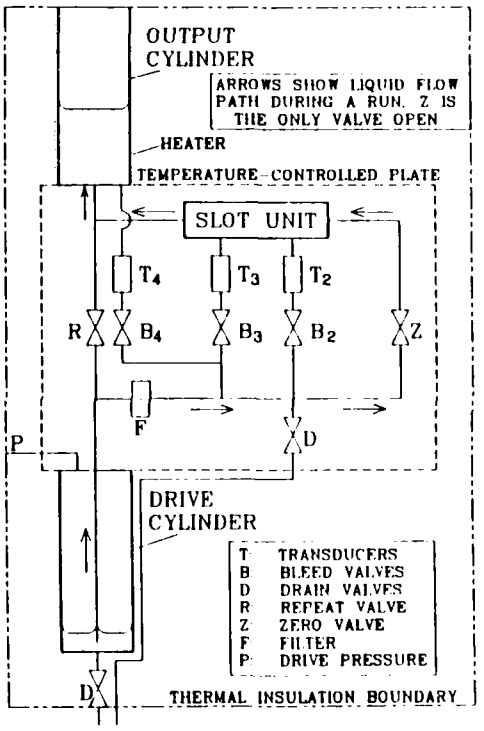


**FIGURE 6** Schematic diagram of the liquid flow system of the high shear rate STRESSMETER. Arrows show the flow path during a run: with Z the only valve open, gas pressure drives the liquid from the drive cylinder through the filter F & slot unit into the output cylinder. The other valves are used for filling, bleeding, & emptying. Heaters on the outer surfaces of an oven & the cylinders are used in conjunction with 8 separate circuits to control temperature. The system is surrounded by thermal insulation.

In the commercial version (22) of the high shear rate STRESSMETER used in the GM/Shell study (1) & in the work reported here, specially made diaphragm-capacitance transducers are used for $T_1$ to $T_4$. $T_4$ is used in a direct-reading mode; its signal is differentiated with respect to time by an analog circuit. The transducer $T_1$

is used as a null indicator in a servo circuit controlling a pressure regulator which supplies compressed air to the electrode side of the transducer at a pressure which is automatically adjusted so as to equal the pressure $P_1$ exerted by the flowing liquid. Similar systems are used with $T_2$ & $T_3$. The 3 liquid pressures $P_1$, $P_2$, & $P_3$ are thereby equilibrated with air pressures. $T_1$, $T_2$, & $T_3$ do not need to be calibrated; their nonlinearity does not matter; they need stable zeros at the working temperature. The air pressures $P_1$ & $P_2$ act on the two sides of a high-linear-range pressure difference transducer $T_5$, whose output gives $P_1-P_2$. Air pressures $P_2$ & $P_3$ are applied to a second similar transducer $T_6$, whose output gives $P_2-P_3$.

Output data read from digital meters are typed into a computer for data evaluation; programs have been written which include differentiations required by the "W-R Equation" (7) & the HPBL Eq.(4); typical die dimensions & output data are given in Table 1.

Fig.6 is a schematic diagram of the complete liquid flow system. Filtered test liquid is forced upwards into the drive cylinder through the lower valve D, which is then closed. With valves R & Z closed, drive pressure applied to the drive cylinder forces the liquid upwards through the bleed valves $B_2$, $B_3$, $B_4$, past the transducers $T_2$, $T_3$, $T_4$, & through the slots in the slot unit. When liquid flowing into the output cylinder is seen to be bubble-free, $B_2$-$B_4$ are closed & Z is opened in order to fill the rest of the die with liquid. During a run, Z is the only valve open.

After a run, the drive pressure is reduced to zero & the valve R is opened to return the liquid to the drive cylinder. Density can also be measured by using the pressure transducer $T_4$ to measure the pressure generated by the head of liquid filling the tube connecting $T_4$ to the base of the output cylinder. A standard liquid of known density is used in a separate similar experiment at the same temperature. A comparison of the two pressure readings gives the required density. An accuracy of the order of 1% or better is attainable; this is more than adequate for calculating Re for use in the STRESSMETER data analysis.

The transducer $T_4$ can be calibrated in a few minutes *in situ* at the working temperature. The outer cylinder is filled with test liquid & all valves are closed. Known air pressures (measured by a Betz micromanometer with a range of 2.5 kPa) are applied to the electrode side of $T_4$ & the $P_4$ readings recorded. The $T_4$ nonlinearity is significant, & a linear second order regression is used to fit the calibration data; about 6 data pairs usually suffice. For the density measurement, $T_4$ can be used solely as a null indicator; the $T_4$ calibration is not needed. One-point calibrations of the pressure difference transducers $T_5$, $T_6$ are made with a mercury manometer.

## MEASUREMENT OF $P^*_f$ & $P^*_N$

Although this section deals only with practical details of the measurement technique, these are far from routine & are essential if reliable multigrade oil data are to be obtained.

For multigrade oils, the average polymer molecular weight is not very high & the elasticity is rather small (compared with that of other polymer solutions for which $N_1$ data are given in the literature); consequently, $P^*_f$, $P^*_N$ & $P^*_e$ are comparable in magnitude. In order to get $P^*_e$ (and hence $N_1$) from the difference $P^*-P^*_f-P^*_N$, it is therefore essential to measure $P^*_f$ & $P^*_N$ accurately. It is reasonable to use the following equations for these quantities:

$$P^*_f = B_1\sigma + B_2\sigma^2 + \ldots + B_M\sigma^M; \qquad (9)$$

$$-P^*_N/\sigma = A_1 Re + A_2 Re^2 + \ldots + A_m Re^m. \qquad (10)$$

The coefficients $B_i$ may vary with temperature and temperature history because differential thermal expansion may cause small relative movements of electrode and transducer case. If the $T_1$ diaphragm deflection gives a negligible change in the die height h, the coefficients $A_i$ should be determined by the detailed shape of the $T_2$ slot edges alone; if these are both perfectly sharp, the dependence of $P^*_N/\sigma$ on Re should agree with that computed (23) for a Newtonian liquid. In any case, $A_i$ should be constants for a given slot unit. We assume that $P^*_N$ can be determined using a Newtonian liquid and then used for non-Newtonian liquids by taking the value of Re at the wall to be equal to that of the Newtonian liquid.

Our present purpose is to determine $A_i$ & $B_i$ experimentally. If in Eq.(10) one changes the independent variable from Re to $\sigma$, the coefficients of the powers of $\sigma$ in the resulting equation will depend on $\eta$. The coefficients $B_i$ in Eq.(9) do not depend on $\eta$. In principle, therefore, one can get $A_i$ & $B_i$ from $P^*(\sigma)$ data at one temperature for two Newtonian liquids of different viscosities. We now consider what values of viscosity $\eta$ to choose.

**METHOD A** - An obvious choice ("Method A") is to take $\eta$ large enough so that Re is sufficiently small for the inertial contribution $P^*_N$ to be negligibly small over the whole $\sigma$ range required, so that $P^*_f = P^*$. Having thus determined $P^*_f$, one can then measure $P^*$ for a Newtonian liquid of smaller $\eta$ & get $P^*_N = P^*-P^*_f$. We have used this method with some success (11), but we now feel that it has certain practical drawbacks: the higher $\eta$ is, the more likely is the liquid to have a small elasticity, the more difficult is the servo system operation, & the more time it takes to change samples.

Using "Bright Stock" ($\eta$ = 1.3 Pa.s) at 20C to get $P^*_f$ & at higher temperatures to get $P^*_N$, values of $A_i$ & $B_i$ were obtained by regressions, & were subsequently used to evaluate $P^*_e(\sigma)$ for an experimental multigrade oil (labelled "UN20" then & "BC30" now) at 50C and 60C. A LODGE STRESSMETER(R) (Serial No.H301) was used. It was found (11, fig.22) that the points fell on a

common curve $P^*_e(\sigma)$ up to, but not above, Re = 15. If the time-temperature superposition principle was valid for this oil, these results suggested that the HPBL eq. was valid up to, but not above, Re = 15; this meant that the STRESSMETER could give values of $N_1$ at 60C (where $\eta$ = 22 mPa.s) for $\dot{\gamma}$ up to, but not above, 3 $10^5 s^{-1}$. The data obtained by Shell (1) with a similar STRESSMETER (Serial No. H302) were thought to be subject to the same restriction Re < 15; extrapolation was used to get $N_1$ values at higher temperatures & shear rates for the journal bearing studies.

Our recent studies (again made with Serial No.H301) cast doubt on the validity of this restriction, show no indication of the existence of a restriction up to Re = 99 (the largest value used to date), & suggest that $N_1$ can in fact be measured up to $\dot{\gamma} = 10^6 s^{-1}$ at 100C. Our previous method of determining $P^*_f$ and $P^*_N$ involved the assumptions that $P^*_e = 0$ for Bright Stock near 20C & that $P^*_f(\sigma)$ is independent of temperature. Our new method makes no such assumptions.

**METHOD B** - Let $P^*_a$ & $P^*_b$ denote values of $P^*$ measured using two Newtonian liquids "a", "b" (preferably at one temperature). It is convenient to choose $\eta$ (in mPa.s) in the range 10-15 for one liquid & 20-25 for the other. There is a greater choice of such liquids which ought to be Newtonian (i.e., $P^*_e = 0$), & so additional tests could be made by comparing results obtained with low-molecular-weight liquids of varied chemical composition. If such comparisons give consistent results, the assumption $P^*_e = 0$ would be supported. Since the coefficients $B_i$ should have the same values for the two liquids, it follows from Eqs.(1), (2), (8)-(10) that, on taking the difference between values of $P^*(\sigma)$ obtained for the two liquids, the $P^*_f$ contributions cancel, leaving the result

$$P^*_b - P^*_a = \sum_{n=1}^{m} A_n (bh/4)^n \{(\rho_a/\eta_a^2)^n - (\rho_b/\eta_b^2)^n\}\sigma^n . \quad (11)$$

It follows that an $m^{th}$ order linear regression analysis with $X = \sigma$ & $Y = P^*_b - P^*_a$ will yield the required values of the coefficients $A_n$. One can then use Eq.(10) for either liquid to determine $P^*_N$ & use the $P^*$ data for either liquid in conjunction with Eq.(1) (with $P^*_e = 0$) to determine $P^*_f$.

**METHOD C** - In practice, the following procedure has been found convenient with Method B. We shall use the term Method C to mean measurements made according to Method B & evaluated as follows. It is convenient to use kPa as units.

<u>1st Regression</u> - Take $X = \sigma$, $Y = P^*_a/\sigma$, & M = 5 (say); determine $G_1, \ldots, G_5$, where

$$P^*_a/\sigma = \sum_{n=1}^{5} G_n \sigma^{n-1} . \quad (12)$$

<u>2nd Regression</u> - Take $Y = \{P^*_b - \sum_{n=1}^{5} G_n \sigma^n\}/\sigma^2$,

$X = \sigma$; determine the coefficients $D_1, \ldots D_4$, where

$$\{P^*_b - \sum_{n=1}^{5} G_n \sigma^n\}/\sigma^2 = \sum_{n=1}^{4} D_n \sigma^{n-1} . \quad (13)$$

The required coefficients $B_1, \ldots, B_5$ are then given by the equations

$$B_1 = G_1, \quad B_n = G_n + D_{n-1}/(1 - R^{n-1}) \quad (n = 2,..,5), \quad (14)$$

where $R := (\rho_b \eta_a^2)/(\rho_a \eta_b^2)$. (15)

$P^*_f$ is now given by Eq.(9) with M = 5.

One could now determine $A_i$ from the above equations by using the result

$$A_n = D_n/(1-R^n)/\{bh\rho_a/(4\eta_a^2)\}^n \quad (n = 1,..4), \quad (16)$$

but it is usually better to increase the Re range by combining $P^*$ data for different liquids & temperatures & to calculate $P^*_N$ from the eq.

$$P^*_N = P^* - \sum_{n=1}^{5} B_n \sigma^n . \quad (17)$$

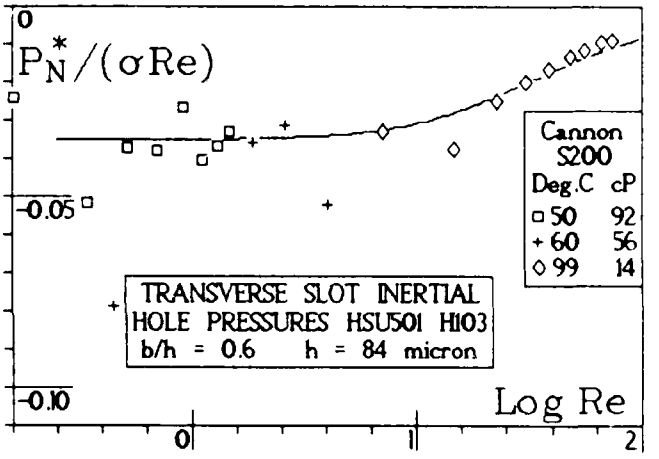


**FIGURE 7** Values of $P^*_N$, the inertial contribution to hole pressure, measured at three temperatures using Method C, agree with numerical simulation (full curve) (23) up to Re = 30.

An illustration of results obtained by Method C as described up to this point is given in fig.7 for a Cannon standard viscosity liquid, "S200", at 50C, 60C, & 99C. The ordinate is $P^*_N/(\sigma Re)$, with $P^*_N$ evaluated by means of Eq.(17) for the individual data points at the three temperatures. The full curve represents results of a numerical simulation (23) with no adjustable parameter being used. It is seen that, although the scatter increases as Re decreases, the measurements & simulation are consistent up to Re = 30; for Re > 30, the measurements lie above the simulation curve. (Another slot unit has given data which lie below, instead of above, the theoretical curve.) Within the scatter, the measurements are seen to be independent of temperature; this was achieved by a prior temperature cycling procedure. Although further experiments with intermediate temperatures (or viscosities) would be desirable for a more thorough test of temperature independence, the results are evidence for the validity of the

present method. The difference between the data points & simulation found for Re > 30 may be due to slot edge imperfections or to errors in σ measurement arising from microbubbles in the test liquid, which had not been degassed. Such errors have been found, particularly at low viscosities & high shear rates (see below).

For later use, it is convenient to fit a polynomial to experimental points such as those shown in fig.7. It is reasonable to omit the few outlying points & to use the following means to obtain a reasonable result at low Re where the scatter is rather large. At low Re, the graph of $P^*_N/(\sigma Re)$ v. log Re shows that, although the scatter is considerable, the experimental points are consistent with the theoretical curve. We may, therefore, use the theoretical low-Re-limiting value -0.035 for $P^*_N/(\sigma Re)$ obtained by several independent simulations (24) & force the polynomial to give this value as Re → 0. This can be achieved as follows.

3rd Regression - Obtain $P^*_N$ values from Eq.(17); take $X = Re^{0.25}$, $Y = -\{P^*_N/(\sigma Re) + 0.035\}/X$; one thus obtains a regression equation

$$-P^*_N/(\sigma Re) = 0.035 + a_2X + .... + a_6X^5, \qquad X = Re^{0.25}. \quad (18)$$

Use of a power such as 0.25 enables one to reduce the order of regression.

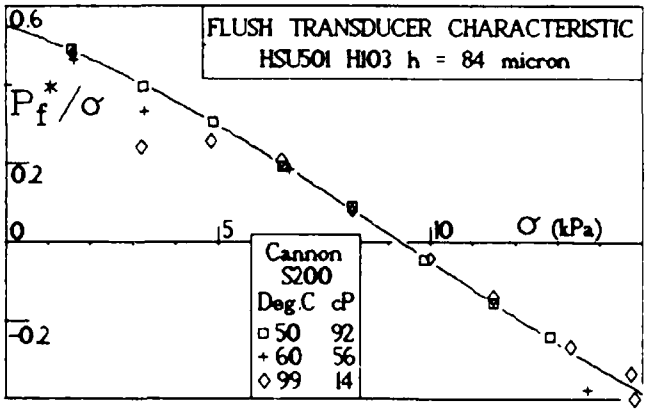


**FIGURE 8** Method C values for the flush transducer finite-width contribution $P^*_f(\sigma)$ are seen to be independent of temperature.

Fig.8 shows a final test of this method made with the same values of P* for S200 at 50C, 60C, & 99C as those used to prepare fig.7. The ordinate represents values of $P^*_f/\sigma$, where $P^*_f$ is determined from $P^*-P^*_N$, with $P^*_N$ evaluated by means of Eq.(18). It is seen that the data for the three temperatures fall on a common curve (within the scatter); the full curve represents the polynomial in Eq.(9), with M = 3. This is evidence of the validity of the present method & shows that, for this transducer & die height, $P^*_f(\sigma)$ is independent of temperature.

We find that $P^*_f(\sigma)$ can vary with temperature after a transducer is first assembled & used; after a few temperature cycles, $P^*_f(\sigma)$ usually settles down to a stable, temperature-independent form (fig.8).

The final result of using Method C (with P* data for two Newtonian liquids) is the determination of values for the coefficients $a_i$ & $B_i$ in the regression equations (9) & (18); typical values are given in the footnote to Table 1.

From P* data for a non-Newtonian liquid, one can then get $P^*_e = P^*-P^*_f-P^*_N$, on using Eqs.(9) & (18) for $P^*_f$ & $P^*_N$; it is assumed that the value of η at the die wall can be used to calculate Re for use in Eq.(18). All data given below were obtained in this way.

## STRESSMETER & TORSIONAL BALANCE RHEOMETER DATA

As a test of our method of measuring $N_1$ & η, we have compared STRESSMETER data with data obtained (25) in the UK on a Torsional Balance Rheometer ("TBR"), an absolute rotational parallel plate rheometer (26, 27) which gives $\dot\gamma$, σ, & $N_1-N_2$ for values of $\dot\gamma$ up to $2\ 10^4 s^{-1}$. Samples were drawn from the same batch of a polymer solution "D2" containing 10.3 wt% of polyisobutylene ("Oppanol B50" from BASF; $M_v$ = 400,000) in decalin. $N_2$ denotes the second normal stress difference in shear flow; in order to calculate $N_1$ from $N_1-N_2$, we used a value 0.1 for $-N_2/N_1$. Values near 0.1 have been obtained (12, 44) at low shear stress for a decalin solution "D1" with higher molecular weight polyisobutylene. The "D2" data comparison is shown in fig.9.

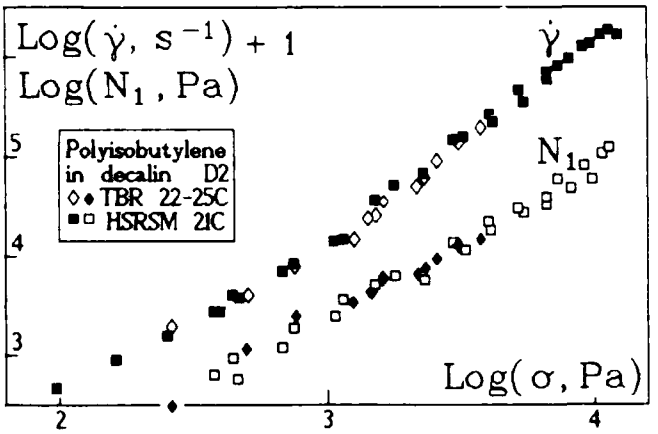


**FIGURE 9** For a polyisobutylene/decalin solution "D2", STRESSMETER & TBR data for η & $N_1$ agree. Over the common $\dot\gamma$ range (300 to 20,700 $s^{-1}$), η decreased from 2 to 0.2 Pa.s, & $N_1/\sigma$ increased from 2 to 4.

It is seen that, within the scatter, there is agreement between the STRESSMETER data & the TBR data over the limited common range of shear stress. The small difference in temperatures used makes no significant difference to the comparison because $-\partial(\ln \eta)/\partial T$ is only 0.01 $K^{-1}$.

The agreement between the data for $\dot\gamma(\sigma)$ obtained with the two instruments suggests that errors due to wall effects, flush transducer diaphragm deflection, entrance & exit effects, & microbubbles were negligible in comparison with the scatter of the data. The agreement between the data obtained for $N_1(\sigma)$ is evidence of the

validity of HPBL Eqs. (1), (3) & (4) but does not, of course, *prove* their validity. There may, for example, be a cancellation of errors, & the scatter in our data may be too great for us to detect errors such as those arising from wall effects: typically, these give differences of about 12% or less in values for viscosity measured in rotational and in capillary viscometers (28) when the capillary surfaces are specially treated.

## STRESSMETER TESTS FOR $\dot{\gamma} > 20{,}700\ s^{-1}$

In attempting to test our method of measuring $N_1$ for $\dot{\gamma} > 20{,}700\ s^{-1}$ (the TBR upper limit) we are faced with the difficulty that there is no other rheometer which can give the required data. Capillary jet thrust has been investigated (21, 29, 30), but the difficulties of data interpretation have not yet been overcome (21); Bernd's oil data (30) for $\dot{\gamma}$ near $10^6 s^{-1}$ are strongly dependent on capillary diameter & are therefore unacceptable; in addition, jet thrusts for Newtonian liquids & multigrade oils differ by only 3% (31).

We must, therefore, make some assumption *in order to test* STRESSMETER measurements up to $\dot{\gamma} = 10^6 s^{-1}$. We shall use the well known *time-temperature superposition* properties which have been established experimentally for a variety of polymeric liquids (32), notably those involving flexible homopolymers (such as polyisobutylene). We recognize that multigrade oils containing block copolymers may not give time-temperature superposition. It is reasonable first to test the method using polyisobutylene solutions and others which exhibit time-temperature superposition. If the tests are positive, one can then assume that the STRESSMETER method will also apply to block copolymer solutions; one should also investigate these using TBR data, although the $\dot{\gamma}$ range would be limited.

We choose the following variables:

*dependent:* $\sigma$, $\sigma_p$, $\sigma_r$, $\sigma_{pr}$, $N_1$, $N_{1r}$, $P^*_e$, $P^*_{er}$;

*independent:* $T$, $\dot{\gamma}_r$. (19)

Here, $\sigma_p := \sigma - \eta_s\dot{\gamma}$ (the polymer contribution to shear stress); $\eta_s$ denotes the solvent viscosity; $\dot{\gamma}_r := \dot{\gamma}a(T)$, where $a(T)$ is a function of the absolute temperature $T$ alone, chosen to give superposition; & $X_r := \rho_o T_o X/(\rho T)$ where $X$ denotes any stress or pressure variable & $\rho_o$ denotes the value of density $\rho$ at $T = T_o$.

Liquids are said to satisfy a *time-temperature superposition principle* in ranges $T_1 < T < T_2$, $\dot{\gamma}_{r1} < \dot{\gamma}_r < \dot{\gamma}_{r2}$ if a function $a(T)$ can be found such that

$$\partial\sigma_{pr}/\partial T = 0 \qquad (20)$$

and

$$\partial N_{1r}/\partial T = 0. \qquad (21)$$

Such equations are satisfied by the Rouse-Zimm theory for dilute polymer solutions (33) when certain model parameters ($h^*$, $N$) are independent of $T$ & by Oettinger's recent development (34) of these theories which gives $\partial\eta/\partial\dot{\gamma}$ nonzero.

In order to test the validity of the HPBL Eq.(3), we shall use only the following form of time-temperature superposition assumption:

*If Eq.*(20) *is valid, then Eq.*(21) *is valid.* (22)

STRESSMETER data given below agree with Eq.(20) & with the equations

$$\partial P^*_{er}/\partial T = 0 \qquad (23)$$

and

$$\partial L^*/\partial T = 0, \qquad (24)$$

where

$$L^* := \frac{\partial \log \sigma_{pr}}{\partial \log \dot{\gamma}_r} \Big/ \frac{\partial \log \sigma_r}{\partial \log \dot{\gamma}_r}. \qquad (25)$$

It follows from Eqs.(20), (22) - (25) that

$$\partial(N_1 - 2nP^*_e)/\partial T = 0, \qquad (26)$$

where

$$n := \frac{\partial \log P^*_{er}}{\partial \log \dot{\gamma}_r} \Big/ \frac{\partial \log \sigma_r}{\partial \log \dot{\gamma}_r}, \qquad (27)$$

in agreement with Eq.(4).

Hence, if TBR & STRESSMETER data show that $N_1 = 2nP^*_e$ at $T_1$ & that the above properties hold for $T_1 < T < T_2$ & $\dot{\gamma}_0 < \dot{\gamma} < \dot{\gamma}_1$, it follows that $N_1 = 2nP^*_e$ at $T_2$, and that *the HPBL Eq.(3) is valid up to a higher shear rate* $\dot{\gamma}_2$, *where*

$$\dot{\gamma}_2 = \dot{\gamma}_1 a(T_1)/a(T_2). \qquad (28)$$

This is the required result. The only *assumption* involved here is Eq.(22), because the range of validity of the remaining Eqs.(20), (23), & (25) can be found from STRESSMETER measurements.

If (as is the case for "D2") the solvent viscosity $\eta_s$ *is negligibly small in comparison* with the solution viscosity $\eta$, then $\sigma_{pr} = \sigma_r$; hence $L^* = 1$ & Eq.(24) is satisfied. For multigrade oils, however, this is not the case: the relative viscosity $\eta_{rel} := \eta/\eta_s$ can vary between about 1.2 & 2; for the oil "BC30" considered below, our measurements show that, while $L^*$ differs significantly from 1, it has no significant dependence on temperature, so that Eq.(24) is satisfied within the scatter of the data. This result may reflect the low $\dot{\gamma}$-dependence of $\eta$.

As an illustration of the above procedure for the case $L^* = 1$, we use the STRESSMETER data for "D2" for the range 21C to 111C shown in fig.10. The lower sets of data points (representing $\sigma_r(\dot{\gamma}_r) = \sigma_{pr}(\dot{\gamma}_r)$) clearly superpose (within the scatter); values of $a(T)$ have been chosen to give this superposition. Thus Eq.(20) is satisfied. The upper sets of data points show, further, that the same values for $a(T)$ also make the data for $P^*_{er}(\dot{\gamma}_r)$ superpose (although the scatter is somewhat larger at low $\dot{\gamma}_r$), showing that Eq.(23) is satisfied. We may, therefore, use the above procedure with $T_1 = 21C$, $T_2 = 111C$, & $\dot{\gamma}_1 = 300\ s^{-1}$; we then find, from Eq.(28), that $\dot{\gamma}_2 = 1.1\ 10^5 s^{-1}$.

Using (22), we have thus shown that the STRESSMETER gives valid $N_1$ data for "D2" up to $1.1\ 10^5\ s^{-1}$ at 111C; here, $\eta = 32$ mPa.s. This is based on the comparison with TBR data at 21C up to $20{,}700\ s^{-1}$ (fig.9); here, $\sigma = 3.7$ kPa. The STRESSMETER data in fig.10 show, however, that $P^*_{er}(\dot{\gamma}_r)$ & $\sigma_r(\dot{\gamma}_r)$ are temperature independent up

to $\dot{\gamma}$ = 2.9 $10^5 s^{-1}$ at 111C (where $\eta$ = 21 mPa.s) & up to $\dot{\gamma}_r$ = 3.9 $10^5 s^{-1}$ with a(T) = 1 at 111C. This gives some reason to believe that the $N_1$ data are reliable up to these shear rates.

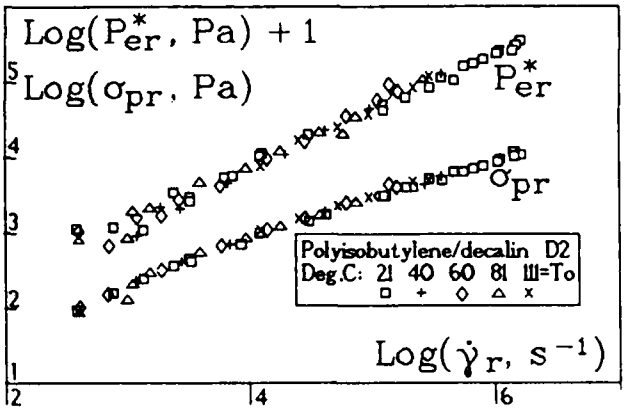


**FIGURE 10** STRESSMETER data for log $P^*_{er}$ (upper points) & log $\sigma_r$ (lower points) for the polyisobutylene solution "D2" featured in fig.9 are seen to satisfy a time-temperature superposition principle over the range 21C to 111C. For this solution, $\sigma_p = \sigma$ to within 1%. The results suggest that transverse slot hole pressure measurements coupled with the HPBL equations can give values of $N_1$ up to $\dot{\gamma}$ = 2.9 $10^5$ $s^{-1}$ (the highest value for the data shown).

To get higher $\dot{\gamma}$ values, the polyisobutylene-decalin solution "D2" was diluted to give an 8.7 wt% solution "D2b". Similar TBR tests on D2b, to be reported elsewhere (35), support the validity of the STRESSMETER method of determining $N_1$ up to $\dot{\gamma}$ = 1.2 $10^6 s^{-1}$ at 99C; here, $\eta$ = 10 mPa.s, $N_1/\sigma$ = 9.7, & Re = 96; thus the previous restriction, Re < 15, is invalid.

## $N_1$ DATA FOR A MULTIGRADE OIL "BC30"

STRESSMETER data for an undegassed multigrade oil (labelled "BC30" in house) are presented in figs.11-14 & Table 1. $N_1$ is too small for TBR measurement, so time-temperature superposition is again used to test our method of measuring $N_1$. $\eta_{rel}$ varies from 1.6 to 1.2, so $\eta_s$ is a significant part of $\eta$ which varies from 40 mPa.s at 40C to 13 mPa.s at 74C, the highest temperature used. The changes in $\eta$ & $\eta_p$ with $\dot{\gamma}$ are about 4% & 50%.

Fig.11 shows that $P^*_{er}$ & most $\sigma_{pr}$ data taken at different temperatures superpose. The deviations of the $\sigma_{pr}$ data at 74C (crosses) at the highest $\dot{\gamma}_r$ are attributed to errors caused by bubble trouble (see below). These outlying points were omitted when a regression was performed to express $\sigma_{pr}(\dot{\gamma}_r)$ as a polynomial; a regression was also used to express $P^*_{er}(\dot{\gamma}_r)$ as a polynomial. The two polynomials were used to evaluate derivatives in order to determine n by means of Eq.(27). The $\sigma_{pr}$ data superposition shown by the lower set of points in fig.11 shows that Eq.(20) is valid, within the scatter.

We find that $\sigma$ data do not superpose when the same function a(T) is used. This is important here, because it is not $\sigma_p$ but $\sigma$ that occurs in the HPBL Eq.(4), & so one might think that $N_1$ data, evaluated by means of Eqs.(3), (4) would not superpose. However, the slopes of the curves $\sigma_r(\dot{\gamma}_r)$ & $\sigma_{pr}(\dot{\gamma}_r)$ have no significant temperature dependence (fig.12); in consequence, Eq.(24) is satisfied, n is independent of temperature, & $N_1$ data (evaluated using Eqs.(3),(4)) do superpose (fig.13). The validity of Eq.(24) is supported by the data of fig.12, in which log $\sigma_r$ is plotted against log $\sigma_{pr}$ with horizontal shifts K(T) chosen to give superposition.

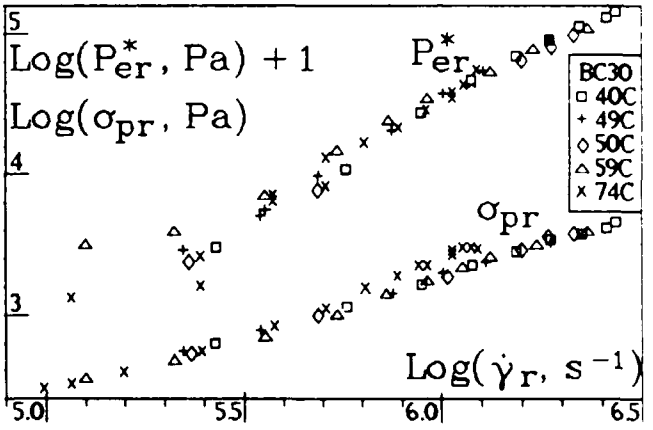


**FIGURE 11** For a multigrade oil at 40C to 74C, STRESSMETER data for $P^*_{er}$ & $\sigma_{pr}$ (the polymer contribution to shear stress) can be superposed by means of a common function a(T). The $\sigma_{pr}$ deviations at 74C at the higher $\dot{\gamma}_r$ are attributed to errors caused by microbubbles in the die.

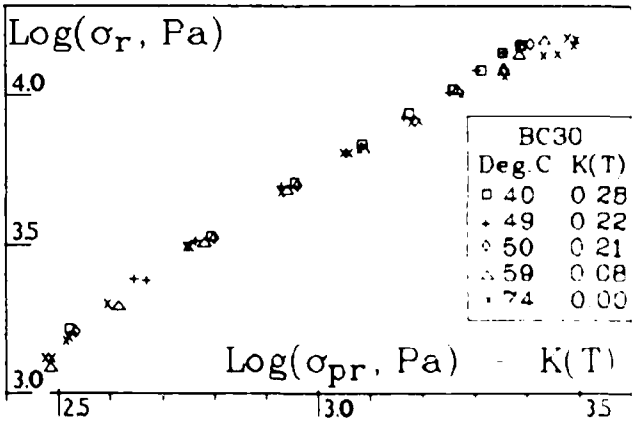


**FIGURE 12** Data for log $\sigma_r$ v. log $\sigma_{pr}$ can be superposed by horizontal shifts of amount K(T). It follows that Eq.(24) is valid. The scatter at the high $\sigma_{pr}$ end is attributed to errors due to microbubbles in the die.

The temperature dependence of K(T) tabulated in fig.12 corresponds to a value of about -0.02 $K^{-1}$ for the relative viscosity temperature coefficient $\partial(\ln \eta_{rel})/\partial T$. This is about 20 times greater in magnitude than values of the

**Table 1: STRESSMETER data for $N_1$ & $\eta$ for a multigrade oil "BC30" at 40C, 59C, & 74C**

| Run No. | Deg. C | DP/SS | HP/SS | FHP/SS | NHP/SS | EHP/SS | Re | Shear stress kPa | Shear rate 1000/s | Viscosity mPas (cP) | N1 kPa | N1/SS | n | Elast. no.E* 10/MPa | W-R corr'n. factor | W-R calc. use^ |
|---|---|---|---|---|---|---|---|---|---|---|---|---|---|---|---|---|
| 1 | 40.0 | 220 | 0.648 | 0.3906 | -.062 | 0.320 | 1.71 | 3.126 | 77.70 | 40.23 | 3.81 | 1.22 | 1.74 | 10.24 | 1.021 | yes |
| 2 | 40.0 | 221 | 0.660 | 0.3910 | -.062 | 0.332 | 1.72 | 3.118 | 77.67 | 40.15 | 3.94 | 1.26 | 1.74 | 10.63 | 1.021 | yes |
| 3 | 39.9 | 225 | 0.641 | 0.4800 | -.028 | 0.189 | 0.75 | 1.529 | 36.04 | 42.44 | 1.23 | 0.81 | 1.93 | 12.36 | 1.026 | yes |
| 4 | 40.1 | 219 | 0.736 | 0.2998 | -.097 | 0.534 | 2.71 | 4.711 | 119.98 | 39.27 | 8.93 | 1.89 | 1.60 | 11.33 | 1.018 | yes |
| 5 | 40.3 | 217 | 0.774 | 0.2040 | -.129 | 0.699 | 3.64 | 6.344 | 161.35 | 39.32 | 14.90 | 2.35 | 1.49 | 11.01 | 1.016 | yes |
| 6 | 40.4 | 214 | 0.740 | 0.1025 | -.164 | 0.802 | 4.74 | 8.034 | 207.13 | 38.79 | 20.67 | 2.57 | 1.41 | 9.98 | 1.014 | yes |
| 7 | 40.6 | 213 | 0.659 | -.0006 | -.193 | 0.853 | 5.71 | 9.711 | 249.92 | 38.86 | 25.59 | 2.64 | 1.34 | 8.78 | 1.013 | yes |
| 8 | 41.4 | 223 | 0.394 | -.2667 | -.271 | 0.931 | 8.53 | 13.875 | 365.36 | 37.98 | 36.98 | 2.67 | 1.21 | 6.71 | 1.011 | yes |
| 9 | 41.3 | 212 | 0.452 | -.2100 | -.261 | 0.924 | 8.17 | 13.007 | 346.03 | 37.59 | 34.88 | 2.68 | 1.23 | 7.10 | 1.011 | yes |
| 10 | 41.0 | 212 | 0.566 | -.1067 | -.227 | 0.900 | 6.90 | 11.399 | 297.80 | 38.28 | 30.65 | 2.69 | 1.28 | 7.90 | 1.012 | yes |

W-R regression: ln (Approximate SR, 1/ms) =-1.005342E-02 (ln SS)^2 + 1.085343 (ln SS) + 3.104561 ; R^2 = .999909 ; SS in kPa.
EHP,N1 regression: ln EHP =-.1592018 (ln SS)^2 + 2.268556 (ln SS) + -2.250128 ; R^2 = .996571 . Density = .868 g/ml.

| | | | | | | | | | | | | | | | | |
|---|---|---|---|---|---|---|---|---|---|---|---|---|---|---|---|---|
| 1 | 59.2 | 226 | 0.675 | 0.4971 | -.082 | 0.260 | 2.26 | 1.218 | 56.11 | 21.71 | 0.64 | 0.52 | 1.25 | 21.31 | 1.044 | yes |
| 2 | 59.3 | 221 | 0.518 | 0.4577 | -.142 | 0.202 | 4.06 | 1.931 | 94.75 | 20.38 | 0.87 | 0.45 | 1.33 | 10.48 | 1.035 | yes |
| 3 | 59.4 | 219 | 0.379 | 0.3891 | -.233 | 0.222 | 7.09 | 3.152 | 159.94 | 19.71 | 1.73 | 0.55 | 1.43 | 7.05 | 1.025 | yes |
| 4 | 59.6 | 217 | 0.271 | 0.2973 | -.329 | 0.303 | 11.00 | 4.754 | 244.66 | 19.43 | 3.85 | 0.81 | 1.52 | 6.38 | 1.016 | yes |
| 5 | 60.1 | 214 | 0.155 | 0.1976 | -.402 | 0.360 | 14.67 | 6.451 | 329.06 | 19.60 | 6.54 | 1.01 | 1.58 | 5.58 | 1.010 | yes |
| 6 | 60.5 | 212 | 0.038 | 0.0963 | -.464 | 0.406 | 18.54 | 8.136 | 415.48 | 19.58 | 9.67 | 1.19 | 1.63 | 4.99 | 1.006 | yes |
| 7 | 61.0 | 207 | -0.136 | -.0178 | -.517 | 0.399 | 22.78 | 9.989 | 510.35 | 19.57 | 12.09 | 1.21 | 1.67 | 4.00 | 1.001 | yes |
| 8 | 60.9 | 206 | -0.261 | -.1292 | -.553 | 0.421 | 26.53 | 11.752 | 597.36 | 19.67 | 15.40 | 1.31 | 1.71 | 3.59 | 0.998 | yes |
| 9 | 61.2 | 199 | -0.471 | -.3344 | -.603 | 0.466 | 34.28 | 14.899 | 764.58 | 19.49 | 22.39 | 1.50 | 1.76 | 3.13 | 0.993 | yes |
| 10 | 61.3 | 207 | -0.369 | -.2318 | -.585 | 0.448 | 30.95 | 13.342 | 687.48 | 19.41 | 18.95 | 1.42 | 1.74 | 3.36 | 0.996 | yes |

W-R regression: ln (Approximate SR, 1/ms) =-3.018947E-02 (ln SS)^2 + 1.143305 (ln SS) + 3.768786 ; R^2 = .9999029 ; SS in kPa.
EHP,N1 regression: ln EHP = .1210471 (ln SS)^2 + .9580033 (ln SS) + -1.471189 ; R^2 = .991825 . Density = .855 g/ml.

| | | | | | | | | | | | | | | | | |
|---|---|---|---|---|---|---|---|---|---|---|---|---|---|---|---|---|
| 1 | 74.2 | 226 | 0.270 | 0.4903 | -.211 | -0.009 | 6.33 | 1.341 | 99.17 | 13.53 | - | - | - | - | 1.044 | yes |
| 2 | 74.2 | 229 | 0.249 | 0.4914 | -.211 | -0.031 | 6.32 | 1.322 | 98.38 | 13.44 | - | - | - | - | 1.044 | yes |
| 3 | 74.6 | 224 | 0.073 | 0.4522 | -.319 | -0.061 | 10.52 | 2.029 | 157.25 | 12.91 | - | - | - | - | 1.032 | yes |
| 4 | 74.5 | 221 | 0.034 | 0.3910 | -.436 | 0.080 | 16.67 | 3.119 | 245.37 | 12.71 | 0.88 | 0.28 | 1.73 | 2.55 | 1.020 | yes |
| 5 | 74.7 | 218 | -0.118 | 0.2975 | -.544 | 0.129 | 25.55 | 4.751 | 374.88 | 12.67 | 2.14 | 0.45 | 1.69 | 2.72 | 1.008 | yes |
| 6 | 75.1 | 214 | -0.290 | 0.1992 | -.605 | 0.116 | 34.77 | 6.425 | 508.57 | 12.63 | 2.56 | 0.40 | 1.67 | 1.81 | 1.000 | yes |
| 7 | 75.4 | 209 | -0.356 | 0.0909 | -.629 | 0.182 | 42.82 | 8.225 | 638.62 | 12.88 | 5.08 | 0.62 | 1.65 | 2.21 | 0.993 | no |
| 8 | 76.1 | 207 | -0.462 | -.0169 | -.636 | 0.191 | 51.98 | 9.974 | 774.83 | 12.87 | 6.39 | 0.64 | 1.63 | 1.91 | 0.988 | no |
| 9 | 76.5 | 204 | -0.531 | -.1116 | -.632 | 0.213 | 58.22 | 11.476 | 879.58 | 13.05 | 8.14 | 0.71 | 1.62 | 1.85 | 0.984 | no |
| 10 | 76.3 | 199 | -0.644 | -.2667 | -.615 | 0.237 | 68.79 | 13.874 | 1051.28 | 13.20 | 10.87 | 0.78 | 1.60 | 1.71 | 0.979 | no |
| 11 | 77.0 | 195 | -0.688 | -.3308 | -.605 | 0.248 | 73.17 | 14.846 | 1121.53 | 13.24 | 12.14 | 0.82 | 1.60 | 1.67 | 0.977 | no |

W-R regression: ln (Approximate SR, 1/ms) =-4.183825E-02 (ln SS) 2 + 1.155627 (ln SS) + 4.223731 ; R^2 = .999953 ; SS in kPa.
EHP,N1 regression: ln EHP =-4.087789E-02 (ln SS)^2 + 1.86902 (ln SS) + -3.437838 ; R^2 = .989662 Density = .845 g/ml.

h = 83.42 microns; r = .0523 cm; b = 49 micron; w = .564 cm; LA = 1.904 cm^2
FHP = flush transducer contribution to hole pressure HP; NHP = inertial contribution to HP. EHP = HP - FHP - NHP. DP = drive pressure.
N1 = 1st normal stress difference; SS = shear stress; EHP = elastic contribution to HP; E* = 100 EHP/(SS) 2 10/MPa; n = d log N1/d log SS.
-NHP/SS/Re = .7 042399E-02 + - .1106126 x + .1384962 x^2 + - .0797017 x^3 + 1.994966E-02 x^4 + -1.818165E-03 x^5, where x = Re^n, n = .25
FHP/SS = .5635465 + -5 401072E-02 SS + -4 199596E-04 SS^2 + 0 SS 3 + 0 SS^4; FHP & SS in kPa. Re = rho*b*h*SR/(4*eta).
SS nonlinear cal. factor dP/dVSS = 1.013593 + -6.586862E-05 dVSS + 1 377292E-08 dVSS^2, P in Pa; dVSS in mV, normalized to 1 at 60 cm mercury.
W-R correction factor = (exact shear rate)/(approximate shear rate); this should be greater than or equal to 1

Note 1 Due to measurement errors in Runs 1-3 at 74C, EHP < 0; $N_1$ is not calculated when EHP < 0
Note 2 Runs 7-11 at 74C are not used for the W-R correction because there is a spurious viscosity increase attributed to errors due to bubble trouble, the oil was not degassed prior to measurement.
Note 3 Approximate solvent viscosities in mPas: 17.8 at 40C; 11 1 at 59C; 9 35 at 74C.

similar quantity $\partial(\ln[\eta])/\partial T$ obtained for dilute solutions of homopolymers (36,37). We do not know the composition of "BC30". It may contain a block copolymer, but, if so, then it is perhaps surprising that time-temperature superposition is found. There is, however, some uncertainty about the values of solvent viscosity. For dilute solutions, these temperature coefficients are approximately equal to the temperature coefficients of the mean square end-to-end distances of polymer molecules (36).

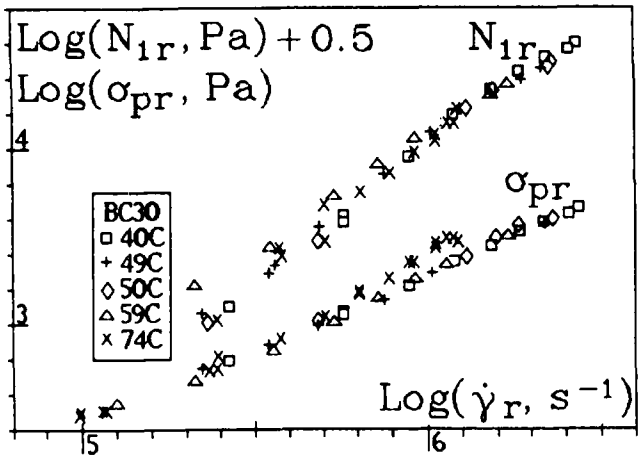


FIGURE 13 STRESSMETER data for $N_1$ and $\sigma_p$ for a multigrade oil "BC30" show time-temperature superposition, except for deviations of $\sigma_p$ at 74C at high $\dot{\gamma}_r$, which are attributed to microbubble errors. The superposition is evidence of the reliability of these measurements up to the highest $\dot{\gamma} = 1.1\ 10^6 s^{-1}$; here, $\eta = 13$ mPa.s at 74C. The highest $\dot{\gamma}_r = 2.7\ 10^6 s^{-1}$.

Using the HPBL Eqs.(3),(4) to evaluate $N_1$, we find that, as expected from figs.11 & 12, the data satisfy the time-temperature superposition condition Eq.(21). Log $N_{1r}(\dot{\gamma}_r)$ & log $\sigma_{pr}(\dot{\gamma}_r)$ data for 40C to 74C are given in fig.13. The superposition supports the view that the STRESSMETER can give valid measurements of $N_1$ for a multigrade oil up to the maximum shear rate used here: $1.1\ 10^6 s^{-1}$ at 74C, where $\eta = 13$ mPa.s. Using $T_o = 74$C, the reduced shear rate $\dot{\gamma}_r$ extends up to $2.7\ 10^6 s^{-1}$. For all these data, $N_1/\sigma < 0.9$, showing that the elasticity is rather small. The greatest value of Re is 83.

For Run 11 at 77C (Table 1), it is seen that $-P^*_e/P^*_N = 0.248/0.605 = 0.41$; this is a "figure of merit" for the STRESSMETER method. For a comparable quantity for the jet thrust method, it is reasonable to use the ratio (elastic thrust)/(inertial thrust); typical values for this ratio for multigrade oils (31) do not exceed about 0.03; this is 14 times smaller than the above value 0.41 for the STRESSMETER method, which is thus the better of the two.

For analyzing the flow of oil in a journal bearing, it is perhaps of interest to use the above data to evaluate the quantity

$$\tau^* := N_1/(2\sigma\dot{\gamma}), \qquad (29)$$

which has the dimension time. One interpretation of this in molecular terms is given by the temporary-junction network theory (38), from which, on using the expressions given for $N_1$ and $\sigma$, we obtain the result

$$\tau^* = \langle\tau^2\rangle/\langle\tau\rangle, \qquad (30)$$

where the averages $\langle..\rangle$ are taken over the distribution of network junction lifetimes $\tau$. Values of $\tau^*$, defined by Eq.(29), are shown in Figure 14, and range from 8 to 0.4 μs.

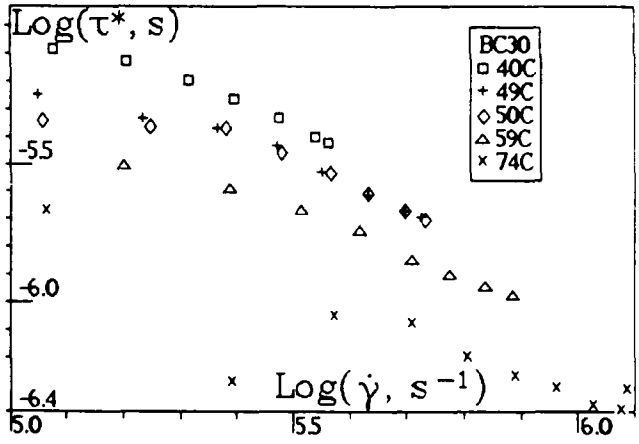


FIGURE 14 Values of log $\tau^*$ v. log $\dot{\gamma}$ for the multigrade oil "BC30" at 40C to 74C evaluated from Stressmeter data. $\tau^* := N_1/(2\sigma\dot{\gamma})$.

The fact that the viscosity is not too strongly dependent on shear rate suggests that either the network theory or the Rouse-Zimm theory might furnish a rough first approximation to a description of the oil; for the Rouse-Zimm theory, in place of Eq.(30) there would be an equation of similar form involving sums over discrete sets of relaxation times and their squares. The choice between these theories would presumably be governed by the value of $c[\eta]$, where c is the concentration and $[\eta]$ the intrinsic viscosity, whose value we do not know. Oettinger's theory (34) gives a better approximation, with $\partial\eta_p/\partial\dot{\gamma}$ not zero.

## VISCOSITY MEASUREMENT FOR $\dot{\gamma} > 10^6 s^{-1}$

Commercial oil viscometers have recently been developed (39) which measure oil viscosities at 150C and $\dot{\gamma} = 10^6 s^{-1}$. In the GM/Shell journal bearing study (1), the maximum $\dot{\gamma}$ was estimated to be $5.6\ 10^6 s^{-1}$. In another study (13), values above $10^7 s^{-1}$ were found in a main bearing during acceleration. It thus appears that $\dot{\gamma}$ values higher than $10^6 s^{-1}$ should be used for current bearing & oil additive research, whatever values may ultimately prove to be best for routine oil testing.

We now describe $\eta$ measurements for $\dot{\gamma}$ up to $5\ 10^6 s^{-1}$ for two Newtonian liquids at 19C: degassed decalin (2.5 cP) & "S6" (a 9 cP Cannon standard).

We use a new "ULTRA-HIGH-SHEAR-RATE VISCOMETER"; this is a STRESSMETER with a new slot unit which has a rigid wall in place of the flush transducer; the die length L, height h, width w, & slot width b are reduced to about 2 mm, 54 or 27 μm, 1.6 mm, & 40 μm, respectively. The remainder of the STRESSMETER (fig.6) is used unchanged; it is convenient to use an annulus inserted in the output cylinder to reduce the free liquid area in order to measure the smaller Q values involved.

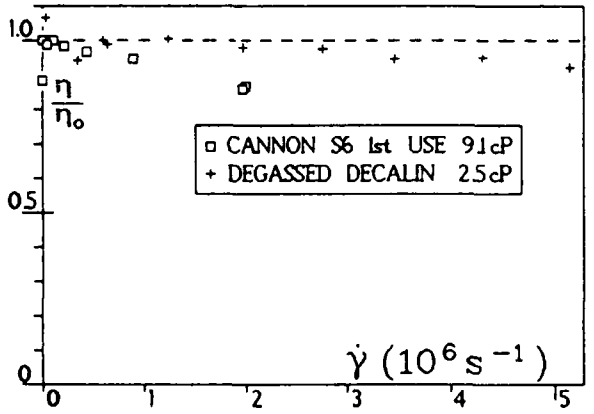


**FIGURE 15** The data points represent values of the viscosity ratio $\eta/\eta_o$ at 19C for two Newtonian liquids measured in the ULTRA-HIGH-SHEAR-RATE VISCOMETER. $\eta_o$ denotes a low shear rate value. For decalin, the shear rate extends to 5 $10^6 s^{-1}$. The small decreases below the expected constant value line are attributed to effects of viscous heating (fig.16).

In fig.15, measured values of $\eta/\eta_o$ v. $\dot{\gamma}$ are shown for the two liquids. $\eta_o$ denotes the low-$\dot{\gamma}$ value. It is seen that, above a $\dot{\gamma}$ value which is different for the two liquids, $\eta/\eta_o$ decreases slightly as $\dot{\gamma}$ increases. For decalin, the greatest shear rate is 5 $10^6 s^{-1}$, & the decrease there is only 8%. This result is encouraging. It is expected that the viscosities of these liquids will not vary with shear rate, & it is probable that the observed small decreases are the effects of non-uniform temperatures generated by the work done on the liquid in driving it through the die ("viscous heating"). To investigate this possibility, we have replotted the data as shown in fig.16.

If (a) the observed decreases are due entirely to effects of viscous heating, (b) the velocity & thermal fields are fully developed at the location of the transverse slots, (c) the flow is laminar, & (d) the walls are isothermal, then the values of viscosity ratio should agree with those given by the exact analysis of Nihoul (40). According to this analysis, the σ value calculated from the "isothermal" Eq.(5) should also be correct for the nonisothermal case & the variation in $\eta/\eta_o$ should be entirely due to the error involved in using the "isothermal" Eq.(6) (with n = 1 for Newtonian liquids) for calculating $\dot{\gamma}$. If we now use $\dot{\gamma}_i$ to denote the isothermal value, given by the eq.

$$\dot{\gamma}_i = 6Q/(wh^2) \quad \text{(isothermal, Newtonian)}, \qquad (31)$$

then the value $\dot{\gamma}$ at the wall in the nonisothermal case is given by the equation

$$\dot{\gamma}/\dot{\gamma}_i = \{1 + (1 - 2Na)^{0.5}\}/2 \quad (Na < 0.5), \qquad (32)$$

where the Nahme number Na is defined by the eq.

$$Na := \beta h^2 \dot{\gamma} \sigma/(36k). \qquad (33)$$

Here, $\beta := -\partial(\ln \eta(\dot{\gamma},T))/\partial T$ (the temperature coefficient of viscosity) & k denotes the thermal conductivity. It then follows that

$$\eta/\eta_o = 2/\{1 + (1 - 2Na)^{0.5}\} \quad (Na < 0.5). \qquad (34)$$

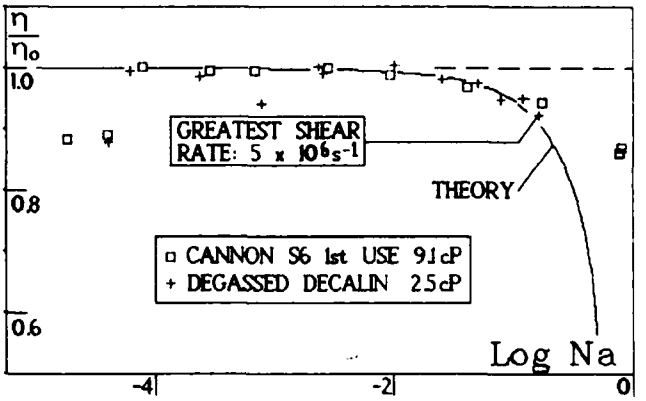


**FIGURE 16** Measured values of the viscosity ratio $\eta/\eta_o$ for two Newtonian liquids plotted versus log (Nahme Number) agree with the theoretical curve for a fully developed thermal field (isothermal walls), except for the two S6 points at the highest value of Na. The agreement suggests that the $\eta/\eta_o$ decrease (which is only 8% at most for decalin) is entirely due to viscous heating & that an appropriate correction can be made by means of the theoretical Eq.(34). This suggests that the ULTRA HIGH SHEAR RATE VISCOMETER can be used to measure viscosities of Newtonian liquids in the 2 to 3 cP region up to $\dot{\gamma}$ = 5 x$10^6 s^{-1}$.

Eq.(34) is represented by the full curve in fig.16, in which $\eta/\eta_o$ is the ordinate & log Na is the abscissa. The points represent single values measured for the two liquids. It is seen that, with the exception of four points which appear to be the result of random scatter and the two S6 points on the right, the data for the two liquids fall on a common curve which agrees with the curve from Eq.(34). The values of the constants for S6 & decalin are given in Table 2.

The agreement shown in fig.16 between the measured points for two different liquids & dies and the theoretical curve suggests that the decrease in measured η values is indeed due to effects of viscous heating up to the greatest $\dot{\gamma}$ used for decalin, namely, 5 $10^6 s^{-1}$. Moreover,

the fact that two liquids having significantly different values for $\eta$, $\beta$, & k (used with dies of different heights) give points on a common theoretical curve suggests that this theory can legitimately be used to correct the measured data (interpreted here by means of isothermal equations) for the effects of viscous heating. Further tests of this suggestion with other liquids & choices of apparatus constants are needed.

The two points for S6 at high Na which lie above the theoretical curve in fig.16 probably reflect a departure from the fully developed thermal field represented by the full curve. A thermal field is closer to being fully developed the smaller is the value of the Graetz Number Gz, defined by the equation

$$Gz := h^3\dot{\gamma}/(6\alpha L), \qquad (35)$$

where $\alpha := k/(\rho C_p)$ denotes the thermal diffusivity. Thermal data are given in Table 2.

TABLE 2 Thermal Data, UHSRV Tests

| | "S6" | Decalin |
|---|---|---|
| Temperature (C) | 19 | 19 |
| Viscosity (cP) | 9.1 | 2.5 |
| Die height (microns) | 53 | 25 |
| (Die length)/(die height) | 54 | 56 |
| Maximum shear rate ($10^6 s^{-1}$) | 2 | 5 |
| $\beta$ ($10^{-2}$ $K^{-1}$) | 4.1 | 1.7 |
| k ($10^{-2}$ N/K/s) | 13 (?) | 11.4 |
| $\rho$ ($kg/m^3$) | 867 | 883 |
| $C_p$ ($10^3$ Nm/kg/K) | 2 (?) | 1.7 |
| $\alpha$ ($10^{-7}$ $m^2/s$) | 75 | 79 |
| Gz at die exit, $\dot{\gamma}_{max}$ | 231 | 119 |

The larger Gz value for "S6" is consistent with the above interpretation of the fact that $\eta/\eta_0$ lies above the theoretical curve for a fully-developed thermal field. It is, perhaps, surprising that, with Gz as large as 119, the decalin data fall near this curve; the thermal field must be far from fully developed (41), but it is the velocity (rather than the thermal) field that governs $\eta/\eta_0$, & the small value of $\beta$ for decalin is therefore relevant here. Numerical simulation will be used to investigate this.

It must be emphasized that these results, encouraging though they are, have been obtained for Newtonian liquids only. For non Newtonian multigrade oils, the viscosity varies significantly (though not greatly) with shear rate; although this variation is often no more than about 30% up to $\dot{\gamma} = 10^6 s^{-1}$, the variation may prove to be greater at the higher shear rates envisaged here.

The well-known slit die analog Eqs.(6), (7) of the Weissenberg-Rabinowitsch calculation of wall shear rate has been derived on the assumption that the test liquid is homogeneous. This assumption is not valid when the effects of viscous heating are significant. It will, therefore, be necessary to see whether an extension of theory can be made (42) which will allow one to calculate wall shear rate from measured slit die data when the viscosity varies with shear rate & the temperature is non-uniform. The fact that, for our ULTRA-HIGH-SHEAR-RATE VISCOMETER, the viscous heating errors are rather small (about 8% for decalin at 5 $10^6 s^{-1}$) gives reason to hope that a perturbation analysis, which treats the two corrections as independent of one another, might be sufficiently accurate for application to multigrade oils under the conditions of journal bearing lubrication.

*Other possible sources of systematic error* in our viscosity measurements include: $\sigma$ errors arising from unequal values of $P^*_N$ at the two slots; variation of $\eta$ with pressure along the die; non-parallelism of the die walls. Further tests are required in order to establish the range of reliability of our measurements, but our estimates show that these errors should be negligible in comparison with the scatter.

For the ULTRA-HIGH-SHEAR-RATE VISCOMETER, the isothermal wall assumption seems reasonable because of the large mass of metal which surrounds the very small die region on all sides. For the STRESSMETER die, however, one wall is a thin stainless steel diaphragm which will conduct heat less effectively than the solid stainless steel wall opposite the flush transducer. The question therefore arises whether both walls should be assumed to be isothermal or whether (as another extreme possibility) one should be assumed to be isothermal & the other adiabatic. Some evidence relevant to this question is given in the next section.

## MEASUREMENTS OF TEMPERATURE RISE

Assuming that the die walls & the liquid entering the die have a uniform temperature field, the effect of viscous heating is to generate a non-uniform temperature field in the flowing liquid. At the early stages of the development of this field, the temperature profile over a cross section normal to the main flow direction has a maximum (41) at some point between the die center & the die wall.

By moving the end of the downstream thermocouple (fig.5) relative to the die wall, we were able to detect changes in the temperature rise measured by the temperature difference thermocouple; values recorded in this way using Probe No.2 are shown in fig.17 for different values of the drive pressure. Measurement errors can occur due to conduction of heat along the thermocouple wires, heat generation by flow disturbance caused by the thermocouple probe, & the need to locate the probe at some distance downstream from the die; the die cross section is too small to allow one to insert a probe in the die, although surface thermocouples on the die wall might be used. The temperature profile at the die exit can be expected to be convected downstream with the liquid to a good extent. Probe No.1, made of thinner wire than that used for Probe no.2, does indeed give higher readings (fig.17) than those given by Probe No.1. This

suggests that heat conduction along probe wires was the dominant error. The data also show that the measurement errors were large in % terms & that the greatest rise recorded was only 2C.

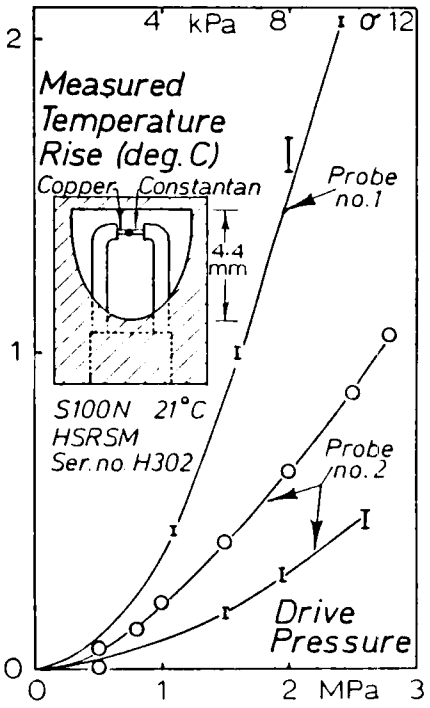


**FIGURE 17** Measured temperature rise due to viscous heating in a Newtonian liquid in a STRESS-METER die. The error due to heat conduction along the thermocouple wires is illustrated by the use of wires of different thickness (Probes 1 & 2). Two sets of readings are shown with Probe 2 in different locations in a downstream cross section.

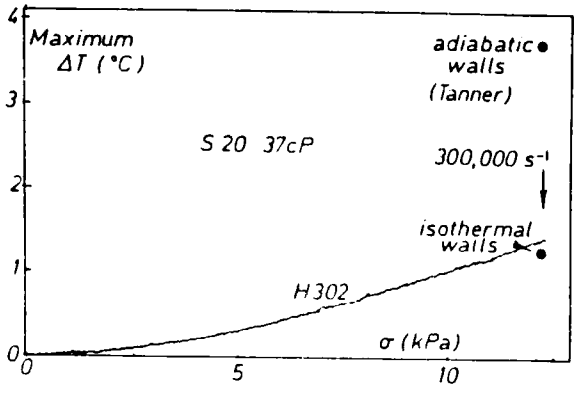


**FIGURE 18** The curve represents the steady increase in temperature rise due to viscous heating as the drive pressure is slowly increased; the probe position in a cross section downstream from the die was previously adjusted to give the greatest reading. The filled circles represent the isothermal & adiabatic limiting values obtained by numerical simulation (43).

Fig.18 shows similar data for a Newtonian liquid (Cannon "S20") taken with the downstream probe position adjusted so as to give the maximum reading. The continuous curve represents a chart recording obtained with a slowly-increasing drive pressure. The two filled circles represent values of the theoretical maximum temperature rise obtained (43) by numerical simulation for our die dimensions (L = 6.8 mm; h = 78 μm) for the two extreme cases in which both die walls are assumed to be isothermal or adiabatic. It is seen that the measured curve falls closer to the isothermal than to the adiabatic point. This is consistent with our expectation that the solid die wall should be approximately isothermal, but the significant measurement errors illustrated in fig.17 suggest that limited weight should be placed on the quantitative agreement between measured temperature rise & temperature rise calculated for the isothermal case. For this reason, we believe that, in order to assess and correct for the effects of viscous heating, more weight can be placed on the variation of $\eta/\eta_0$ with $\dot{\gamma}$ & its comparison with the theoretical result (fig.16).

## BUBBLE TROUBLE

The viscosity data shown in figs.15 & 16 for the lower-viscosity liquid (decalin) were obtained after the decalin had been thoroughly degassed by slow filtration (a few seconds per drop) into a high vacuum obtained with a backing pump. Use of undegassed decalin was found to give anomalous data, with the measured values of $\eta$ passing through a maximum as $\dot{\gamma}$ was increased. Degassing by use of a high vacuum without filtration was found to be inadequate, even when ultrasonics were used.

Fig.19 shows data from the first use of an undegassed Cannon standard viscosity liquid "S3" (3.9 cP at 20C). Data were taken with $\dot{\gamma}$ increasing. The values of $\eta/\eta_0$ for points at the lower $\dot{\gamma}$ values (below 1.7 $10^5 s^{-1}$) give a standard deviation equal to 0.95% of the mean value. This is a measure of the viscometer performance. The anomalous increase found at larger $\dot{\gamma}$ values is not fully understood. We conjecture that somehow the passage of test liquid through zones of large pressure gradient causes agglomeration of microbubbles (already present in the liquid) to an extent that, when the liquid reaches the die, some of these bubbles have sizes comparable with the die height. These bubbles then cause unwanted changes in the pressure gradient near the transverse slots & hence cause errors in the measurement of $\sigma$. We have no direct evidence to support this conjecture, except possibly the observations (a) that thorough degassing eliminates, or very substantially reduces, the stream of bubbles observed (above a certain flow rate) in the liquid flowing into the output cylinder & (b) that, on a succession of 10 runs at one high shear rate, the "S3" viscosity anomaly became less pronounced (as one would expect because passage through the instrument removed some gas from the liquid).

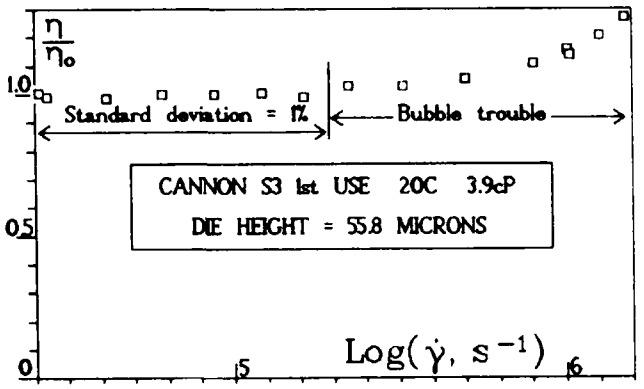


FIGURE 19 For $\dot{\gamma} > 2\ 10^5 s^{-1}$, viscosity measurements show an anomalous increase attributed to the presence of microbubbles of a size comparable with the die height. The liquid was not degassed prior to use. Each point represents one measurement. For the set of 7 points taken at the lower values of shear rate ($\dot{\gamma} < 1.7\ 10^5 s^{-1}$), the standard deviation of $\eta/\eta_o$ is equal to 0.95% of the mean. $\eta_o$ denotes the mean value of $\eta$ for these points.

It is surprising that microbubbles should grow in a region in which the pressure is above atmospheric. Although negative pressures do occur at the die exit at the higher shear rates (because of the Bernoulli pressure), the pressures are estimated to be always above atmospheric at the slots, & this has been checked by direct measurement. Negative pressures, with concomitant bubble formation, at the die exit should not cause errors in our measurements. It appears, therefore, that the effects of pressure gradients in the flow path leading to the transverse slots must outweigh the effect of having the pressures above atmospheric. This is not too surprising when one considers that the greatest drive pressures used (about 500 psi) are small compared with pressures (estimated to be about 7000 psi) required to force all microbubbles into solution; the value 7000 psi is obtained from the known value of 16000 psi for water (45) on the assumption that the effect is surface-tension dominated.

The Cannon liquids are standards when they contain the equilibrium amount of dissolved gas, but not when degassed. For die height measurement, one must, therefore, use undegassed standard liquids only at the lower $\dot{\gamma}$ values where bubble trouble is absent.

If our suggested explanation is correct, it is to be expected that rotational viscometers would not experience similar problems because they do not have significant pressure gradients. In loaded journal bearings, on the other hand, there are large pressure gradients, & so it is natural to wonder whether bubble agglomeration occurs with any significant effect in the *positive*-pressure zone. In the negative-pressure zone, generation of large bubbles (cavitation) is well known.

## CONCLUSIONS

1. 1986 journal bearing oil film thickness measurements (1,13) establish the need for obtaining viscosity & shear (not bulk) elasticity data for multigrade oils at shear rates up to at least 6 $10^6 s^{-1}$.

2. A new commercially available slit-die rheometer, the LODGE STRESSMETER(R) FOR HIGH SHEAR RATES, is shown to be capable of giving such data at shear rates up to $10^6 s^{-1}$.

3. Data for one oil give values of an oil time constant $\tau^*$ as low as 4 $10^{-7}$s.

4. Before measurement, oils should be degassed by slow filtration into a high vacuum in order to avoid errors due to microbubbles.

5. First results with a smaller die suggest that viscosities of the order 2 cP can be measured at shear rates up to 5 $10^6 s^{-1}$.

## ACKNOWLEDGEMENTS

The STRESSMETER was developed with the help of my former graduate students Professors K. Higashitani, D. G. Baird, Drs L. de Vargas & P. P. Tong with financial support from the National Science Foundation (grants GK-15611, ENG 75-18397, GK-35549X, & CME-7824180). The high shear rate version was developed at the request of Dr D. W. Brownawell with financial support from Exxon Chemical Co. The help of Douglas H. Hutchins in designing & constructing the electronics & of Rich Williams in precision machining is gratefully acknowledged. "BC30" Oil base stock viscosity data were kindly provided by Dr R. B. Rhodes (Shell Development Co.). Financial support is gratefully acknowledged from E. I. Du Pont de Nemours & Co. through Polymer Science & Engineering grants to the Rheology Research Center, & from the U.S. Army Research Office through contracts DAAG29-84-K-0046 to me & DAAL-03-86-K-0174 to the Engine Research Center. Prof. K. Walters & Mr F. S. R. Al-Hadithi provided TBR data. Professor A. B. Metzner & Dr S. W. Rein kindly commented on a draft of this paper. Referees' comments & discussions with Professors W. O. Winer, R. K. Prud'homme & Dr M. H. Wagner are gratefully acknowledged. Tabulated values of inertial hole pressures from numerical simulation were kindly provided by Professor B. A. Finlayson. Numerical simulations for temperature fields were generously made by Professor R. I. Tanner.

## NOMENCLATURE

| | |
|---|---|
| $\dot{\gamma}$, $\sigma$ | Wall shear stress & shear rate |
| $N_1$, $N_2$ | 1st & 2nd normal stress differences |
| $\tau^*$ | $N_1/(2\sigma\dot{\gamma})$ |
| $P_1, P_2, P_3$ | Measured pressures, fig.4 |
| $P^*$ | $P_1 - P_2$ ("hole pressure") |
| $P^*_f$ | Finite width contribution to $P^*$ |
| $P^*_e, P^*_N$ | Elastic & inertial contributions to $P^*$ |
| $n$ | $d(\log P^*_e)/d(\log \sigma)$ |
| h, w | Height, width: slit die cross-section |
| z, L | Slot separation & die length |
| b | Slit width |
| $\dot{\gamma}_1$ | $\dot{\gamma}$ calculated from iso-thermal equation |
| T | Absolute temperature |
| $\rho$, $\rho_o$ | Densities at temperatures T, $T_o$ |
| a(T) | Time-temperature shift function |
| $\eta$, $\eta_s$ | Solution & solvent viscosities |
| $\eta_{rel}$ | $\eta/\eta_s$ (relative viscosity) |
| $\eta_o$ | Value of $\eta$ at low shear rates |
| $[\eta]$ | Intrinsic viscosity |
| c | Polymer concentration |
| Re, X | $\rho bh\dot{\gamma}/(4\eta)$, $(Re)^{0.25}$ |
| $\sigma_p$ | $\sigma - \eta_s\dot{\gamma}$ |
| $\dot{\gamma}_r$ | $\dot{\gamma}a(T)$ ("reduced shear rate") |
| $X_r$ | $\rho_o T_o X/(\rho T)$ for $X = \sigma, \sigma_p, N_1, P^*_e$ |
| Na, Gz | $\beta h^2\dot{\gamma}\sigma/(36k)$, $h^3\dot{\gamma}/(6aL)$ |
| k, *a* | Thermal conductivity & diffusivity |
| $C_p$ | Heat capacity |
| $\beta$ | $-\partial(\log \eta(\dot{\gamma},T))/\partial T$ |
| $a_i, A_i, B_i$ | Coefficients in Eqs.(18),(10),(9) |
| $D_i, G_i$ | Coefficients in Eqs.(13),(12) |
| $P^*_a, P^*_b$ | $P^*$ for Newtonian liquids "a", "b" |
| R | $(\rho_b\eta_a^2)/(\rho_a\eta_b^2)$ |
| Q, $n$ | Flow rate, $d(\log Q)/d(\log \sigma)$ |
| $L^*$ | Defined by Eq.(25) |
| MW | Molecular weight |
| $M_v$ | Viscosity-average MW |
| A := B | A is *defined* by the Eq. A = B |

## REFERENCES


1. Bates, T. W., B. Williamson, J. A. Spearot C. K. Murphy, SAE Paper No.860376 (1986).
2. Cameron, A. *J. Inst. Petrol. Tech.* **40**, 191 (1954).
3. Okrent, E. H. *ASLE Trans.* **4**, 97 (1961).
4. Tanner, R. I. *ASLE Trans.* **8**, 179 (1965).
5. Davies, M. J. & K. Walters in *"The Rheology of Lubricants"* (ed. T. C. Davenport, John Wiley & Sons, New York, 1973), p.65.
6. Ballal, B. Y. & R. S. Rivlin, *Trans. Soc. Rheol.* **20**, 65 (1976).
7. Lodge A. S. *"Body Tensor Fields in Continuum Mechanics"* (Academic Press, 1974).
8. Bird, R. B., R. C. Armstrong & O. Hassager, *"Dynamics of Polymeric Liquids"* Vol.1, 2nd ed.(John Wiley & Sons, New York, 1987)p.130.
9. Spearot, J. A., private commun. (1986).
10. Oliver, D. R., private commun. (1987).
11. Lodge, A. S., *Chem. Engr. Commun.* **32**, 1 (1985).
12. Alvarez, G. A., A. S. Lodge & H.-J. Cantow, *Rheol. Acta* **24**, 368 (1985).
13. Schilowitz, A. M., & J. L. Waters, SAE Paper No.861561 (1986).
14. Tong P. P., Ph.D. Thesis, Univ. of Wis.-Madison (1980).
15. Lodge, A. S., in *"Physical Principles of Rheological Measurement"* (ed. Collyer & Clegg, Elsevier Sci. Publ., London, 1987), Ch.11.
16. Higashitani, K. & W. G. Pritchard, *Trans. Soc. Rheol.* **16**, 687 (1972).
17. Baird, D. G., *Trans. Soc. Rheol.* **19**, 147 (1975).
18. Tanner, R. I. & A. C. Pipkin, *Trans. Soc. Rheol.* **13**, 471 (1979).
19. Malkus, D. S., & M. F. Webster, *J. Non-Newtonian Fluid Mech.* **25**, 93 (1987).
20. Sugeng, F., N. Phan-Thien & R. I. Tanner, submitted (1987) to *J. Rheol.*
21. Walters, K. *"Rheometry"* (Chapman & Hall, 1975), Eq.(5.27).
22. The Bannatek Company, Inc., P.O.Box 5472, Madison, WI 53705; tel.(608)238-8322.
23. Jackson, N. R. & B. A. Finlayson, *J. Non-Newt. Fluid Mech.* **10**, 55 (1982).
24. Lodge, A. S., *J. Rheol.* **27**(5), 497 (1983).
25. Lodge, A. S., T. S. R. Al-Hadithi, & K. Walters, *Rheol. Acta* (in press).
26. Walters, K. *Proc. VIIth. Int. Cong. Rheol.* (ed. Kubat, Chalmers Inst.Tech., Gothenburg, 1976) 147.
27. Binding D. M. & K. Walters, *J. Non-Newt. Fluid Mech.* **1**, 277 (1976).
28. Cohen, Y. & A. B. Metzner, *J. Rheol.* **29**(1), 67 (1985).
29. Harris, J., *Nature* **190**, 993 (1961).
30. Bernd, L. H., *J. Lub. Tech.* (July 1986), 561.
31. Oliver, D. R. & M. Shahidullah, *J. Non-Newtonian Fluid Mech.* **8**, 177 (1981).
32. Markovitz, H., *J. Polymer Sci., Symposium No.50*, 431 (1975).
33. Lodge, A. S. & Yeen-jing Wu, *Rheol. Acta* **10**, 539 (1971).
34. Oettinger, H. C., *J. Chem. Phys.* **84**, 4068 (1986); Univ. Wis.-Man. Rep. RRC 109 (1986).
35. Lodge, A. S., T. S. R. Al-Hadithi, & K. Walters, *J.Rheol.* (to be submitted).
36. Flory, P. J., A. Ciferri, & R. Chiang, *J. Amer. Chem. Soc.* **83**, 1023 (1961).
37. Treloar, L. R. G., *"The Physics of Rubber Elasticity"*, 3rd ed., (Clarendon Press, Oxford, 1975) p.300.
38. Lodge, A. S., *Trans. Faraday Soc.* **52**, 120 (1956).
39. Tannas Co., P.O.Box 327, Midland, MI 48640.
40. Nihoul, J. C. J., *Ann. Soc. Sci. Bruxelles* **85**,I,18 (1971).
41. Winter, H. H., *Advances in Heat Transfer* **13**, 205 (1977); fig.8 (with $Z = Gz^{-1}$).
42. Kamal, M. R., & H. Nyun, *Polymer Eng. & Sci.* **20**, 109 (1980).
43. Tanner, R. I., private commun. (1984).
44. Walters, K. *IUPAC Macro 83 (Bucharest)*, 1983 Part 2, 227.
45. Newton Harvey, E., W. D. McElroy, & A. H. Whiteley, *J. Appl. Phys.* **18**, 162 (1947).

END
DATE
FILMED
4-88
DTIC